

AD-A039 185

NAVAL POSTGRADUATE SCHOOL MONTEREY CALIF

F/G 13/1

EFFECTS OF GRAVITY ON GAS-LOADED VARIABLE CONDUCTANCE HEAT PIPE--ETC(U)

MAR 77 M D KELLEHER

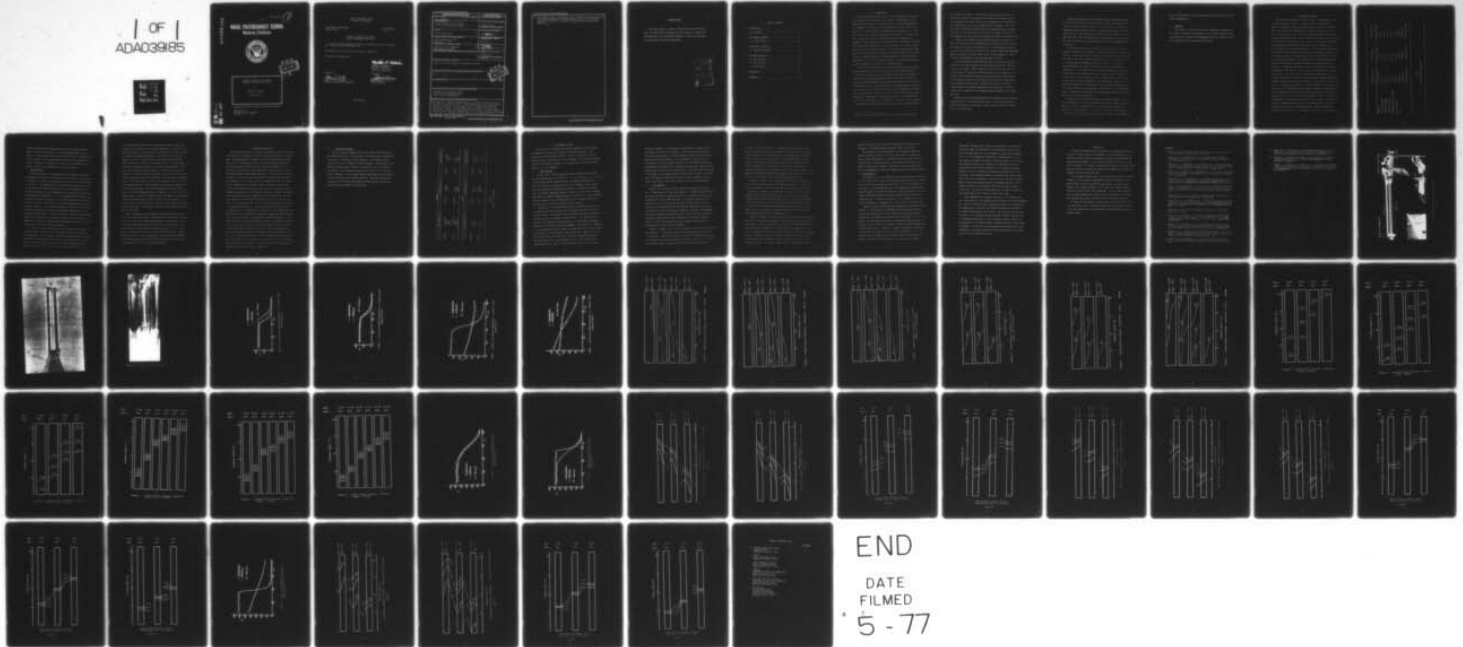
NSF-AG-496

UNCLASSIFIED

NPS-69KK77031

NL

1 OF 1
ADA039185



END

DATE
FILMED
5-77

AD A 039185

NPS-69Kk77031

2

NAVAL POSTGRADUATE SCHOOL

Monterey, California



DDC
MAY 10 1977
C

EFFECTS OF GRAVITY ON GAS-LOADED
VARIABLE CONDUCTANCE HEAT PIPES

by

Matthew D. Kelleher

25 March 1977

Approved for public release; distribution unlimited.

Prepared for:
National Science Foundation
Washington, D.C. 20550

AD No. 1
DDC FILE COPY

NAVAL POSTGRADUATE SCHOOL
Monterey, California

Rear Admiral Isham Linder
Superintendent

J. R. Borsting
Provost

EFFECTS OF GRAVITY ON GAS-LOADED
VARIABLE CONDUCTANCE HEAT PIPES

The work reported herein was supported by the National Science Foundation,
Heat Transfer Program, Washington, D.C.

Reproduction of all or part of this report is authorized.

This report was prepared by:

Matthew D. Kelleher

MATTHEW D. KELLEHER
Associate Professor of
Mechanical Engineering

Reviewed by:

Allen E. Fuhs

ALLEN E. FUHS, Chairman
Mechanical Engineering Department

Released by:

Robert Fossum

ROBERT FOSSUM
Dean of Research

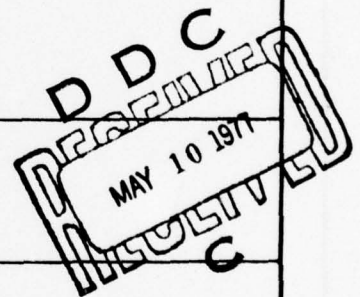
NPS-69Kk77031

REPORT DOCUMENTATION PAGE		READ INSTRUCTIONS BEFORE COMPLETING FORM
1. REPORT NUMBER NPS-69KK 77031	2. GOVT ACCESSION NO.	3. RECIPIENT'S CATALOG NUMBER
4. TITLE (and Subtitle) Effects of Gravity on Gas-Loaded Variable Conductance Heat Pipes		5. TYPE OF REPORT & PERIOD COVERED Final, FY75-76
7. AUTHOR(s) Matthew D. Kelleher		6. PERFORMING ORG. REPORT NUMBER
9. PERFORMING ORGANIZATION NAME AND ADDRESS Naval Postgraduate School Monterey, CA 93940 Code 69KK		8. CONTRACT OR GRANT NUMBER(s) NSF Grant #AG-496
11. CONTROLLING OFFICE NAME AND ADDRESS National Science Foundation Washington, D.C. 20550 Heat Transfer Program		10. PROGRAM ELEMENT, PROJECT, TASK AREA & WORK UNIT NUMBERS 12 6/P.
14. MONITORING AGENCY NAME & ADDRESS (if different from Controlling Office)		12. REPORT DATE 25 March 1977
		13. NUMBER OF PAGES 62
		15. SECURITY CLASS. (of this report) Unclassified
		15a. DECLASSIFICATION/DOWNGRADING SCHEDULE
16. DISTRIBUTION STATEMENT (of this Report) Approved for public release, distribution unlimited		
17. DISTRIBUTION STATEMENT (of the abstract entered in Block 20, if different from Report) Final rept. for FY 75-76,		
18. SUPPLEMENTARY NOTES		
19. KEY WORDS (Continue on reverse side if necessary and identify by block number) Heat Pipes, Gas-Loaded Heat Pipes Variable Conductance Heat Pipes, Liquid Crystal Thermography		
20. ABSTRACT (Continue on reverse side if necessary and identify by block number) The effects of gravity on the operation of gas-loaded variable conductance heat pipes have been investigated. Experimental results have been obtained for three heat pipes (1.6 cm, 2.5 cm and 5 cm diameter) operating with methanol or Freon 113 as the working fluid and krypton or helium as the control gas. Results show that gravity tends to distort the axial temperature profiles on the small diameter pipe. For the large diameter pipe gravity has the effect of causing a stratification of the working fluid and		

DD FORM 1473
1 JAN 73EDITION OF 1 NOV 65 IS OBSOLETE
S/N 0102-014-6601

SECURITY CLASSIFICATION OF THIS PAGE (When Data Entered)

251 450

over
mt

20. non-condensable gas. These results seem to indicate that in certain cases the presently available design procedure will have to be modified to account for the effects of gravity on variable conductance heat pipe operation.

ACKNOWLEDGEMENT

The author wishes to thank Mr. Thomas Christian and Mr. George Bixler for their skillful assistance in the fabrication, assembly and instrumentation of the experimental apparatus, and Mrs. Arlea Morgan for her patience in typing the manuscript.

ACCESSION for		
WTIS	White Section	<input checked="" type="checkbox"/>
G.C.	Buff Section	<input type="checkbox"/>
UNANNOUNCED		<input type="checkbox"/>
JUSTIFICATION.....		
BY		
DISTRIBUTION/AVAILABILITY CODES		
Dist.	AVAIL.	and/or SPECIAL
A		

TABLE OF CONTENTS

1. INTRODUCTION 7
 1.1 Objective 10

2. EXPERIMENTAL APPARATUS 11
 2.1 Liquid Crystals 13

3. EXPERIMENTAL PROCEDURE 15
 3.1 Operating Procedure 16

4. EXPERIMENTAL RESULTS 18
 4.1 Heat Pipe No. 1 18
 4.2 Heat Pipe No. 3 19
 4.3 Heat Pipe No. 2 21

5. CONCLUSIONS 23

REFERENCES 24

1. INTRODUCTION

The conventional heat pipe with its ultra high conductance has made great advances in solving many of the problems of temperature control. Basically, the heat pipe is a passive device - its operating temperature is determined by the source and sink temperatures and the heat load imposed on it. Source temperature and heat load are coupled, i.e., if the heat load varies, the source temperature will also vary. In many situations, such as the cooling of sensitive electronic equipment, it is desirable to have a stable source temperature under conditions of varying heat load or sink temperature. The introduction of the variable conductance heat pipe has provided a means of effectively achieving source temperature stabilization under conditions of varying heat load or sink temperature. Several techniques have been proposed for achieving variable conductance, but of all the proposed methods, the one which has received the most attention is the use of a noncondensable gas.

Marcus [1]* has provided an excellent discussion of all the proposed control mechanisms and particularly the use of noncondensable gases. In recent years a great deal of work has been done in the development of gas loaded variable conductance heat pipes [2-8]. Most of this work, however, has been concerned with heat pipes operating in the zero gravity environment of space. During operation of a gas-controlled heat pipe, the flow of working fluid vapor tends to sweep the noncondensable gas toward the condenser end of the heat pipe where it collects and forms a gas plug. This plug of non-condensable gas blocks a portion of the condenser and very little vapor reaches it. Consequently, this portion of the condenser is unavailable for condensation and the effective heat transfer area of

* Numbers in brackets indicate references listed in the Bibliography.

the condenser is reduced. If the thermal load to the heat pipe is increased, the effect is to increase the pressure and the mass-flow rate of the working-fluid vapor. This, in turn, compresses the noncondensable gas reducing the volume of the condenser which it occupies. This then increases the effective condenser area, thus accommodating the increased heat load. On the other hand, if the load on the pipe is reduced, the noncondensable gas will expand, thus reducing the effective condenser area.

Inherent in the design of gas-controlled variable conductance heat pipes is the necessity for understanding the interaction between the working-fluid vapor and the noncondensable gas. An adequate design implies the ability to predict the location of the interface between the vapor and gas as a function of the heat load, source, or sink temperature and any of the other parameters of the pipe which might be varied.

The first analytical model which was used in the design of gas-controlled [9] heat pipes assumes that the interface between the vapor and the gas is very sharp. Axial conduction in the pipe wall and mass diffusion between the vapor and noncondensable gas are both neglected. Although the qualitative predictions of this so-called flat front theory are substantially correct, the quantitative results differ significantly from experimental observations. Specifically, the flat front theory underestimates the operating temperature of the heat pipe. The major source of error appears to be in neglecting axial conduction in the heat pipe wall.

Rohani and Tien [10] have analyzed the two dimensional heat and mass transfer process in the gas-loaded heat pipe. Their analysis neglects axial conduction in the pipe wall but does include the effects of radial flow in the vapor space.

Edwards and Marcus [11] have formulated an improved analytical model to predict the performance of gas-loaded heat pipes. This analysis includes the effects of axial conduction in the pipe wall, as well as one dimensional binary diffusion between the working fluid vapor and the non-condensable gas. The predications of this diffuse front theory seem to agree quite well with the experimental results obtained from a gas-loaded heat pipe using water as the working-fluid and air as the noncondensable control gas.

The design procedures and analytical tools which have so far been developed to predict the performance of gas loaded heat pipes neglect the effects of gravity on the heat and mass transfer processes within the pipe. This leads to the tacit assumption that the vapor-gas diffusion process is for the most part one dimensional and that, except for the effects on capillary pumping in the wick, the diffusion process is independent of orientation. The experiments which are usually performed to confirm the diffuse front theory usually consist of measuring the axial temperature profile along the pipe surface by means of thermocouples. This procedure assumes that the surface temperature of the pipe gives a measure of the saturation temperature of the working fluid and thereby an indication of its partial pressure and concentration. The placement of the thermocouples along a single axial line assumes that the vapor-gas concentration profile within the pipe is one dimensional.

The diffuse front theory has produced an extremely powerful tool for use in the design of gas-loaded variable conductance heat pipes. However, there still exist situations where one could be led to question the accuracy of the predictions of the diffuse front theory. The situation in which the molecular weights of the working fluid and the non-condensable

gas are very different is one in which effects of gravity must be given careful consideration.

1.1 Objective

The objective of this work has been to investigate experimentally the effects of gravity on the operation of gas-loaded, variable conductance heat pipes in which the non-condensable gas and the working fluid are of significantly different molecular weights.

2. EXPERIMENTAL APPARATUS

Three heat pipes have been built and tested. The dimensions of each heat pipe are given in table I. Each heat pipe is equipped with two pressure transducers, one at the evaporator end and one at the condenser end. The heat pipes are equipped with a precision bellows seal vacuum valve at the evaporator end. This is to facilitate loading with working fluid or noncondensable gas. At the condenser end each heat pipe is fitted with an "O-ring" sealed bleed screw. This is to facilitate the elimination of any extraneous noncondensable gases which might be brought into the heat pipe while filling with working fluid. Each heat pipe was mounted on a frame which would permit the pipe to be rotated through an angle of 180° so that the position of the pipe could be set from horizontal to vertical or any position in between. Each heat pipe has 24 surface thermocouples spaced at 5 cm. intervals along the adiabatic and condenser-reservoir sections. In addition, each heat pipe has two stainless steel sheathed thermocouples which penetrate 1.25 cm. into the evaporator and condenser of each pipe. The 2.5 cm. and 5 cm. diameter heat pipes have 6 extra surface thermocouples placed at 90° angular increments around the circumference of the pipe at two axial positions, 30.5 cm. and 76.2 cm. from the end of the condenser respectively. The heater assembly for each heat pipe consists of 3 mm. Nichrome resistance heater ribbon which has been painted with high temperature electrically insulating varnish and then wrapped around the full 30.5 cm. length of the evaporator section. The evaporator and adiabatic sections were insulated with several layers of thermal insulation. Thermocouples were placed between the layers of insulation to measure the heat loss through the insulation. Power to the heater is furnished by a regulated D.C. power supply. The current in the heater is

	Heat Pipe No. 1	Heat Pipe No. 2	Heat Pipe No. 3
Material	Stainless Steel	Stainless Steel	Stainless Steel
Outside Diameter	1.6 cm	2.5 cm	5. cm
Evaporator Length	30.5 cm	30.5 cm	30.5 cm
Adiabatic Length	15. cm	15. cm	15. cm
Condenser-Reservoir Length	107. cm	107. cm	107. cm
Wall Thickness	0.9 mm	0.5 mm	0.5 mm
Wick	4 Wraps of 150 mesh SS woven wire cloth	5 Wraps of 120 mesh SS woven wire cloth	5 Wraps of 120 mesh SS woven wire cloth

TABLE I

Heat Pipe Design Details

obtained by measuring the voltage across a stable precision resistor placed in series with the heater. All the instrumentation is read by means of a Hewlett-Packard 2010C Data Acquisition System. Further details of the construction of the experimental heat pipes can be found in the Theses of Humphries [12], Nayden [13], Batts [14], and Owendoff [15]. Figures 1,2 and 3 are photographs of the three heat pipes.

2.1 Liquid Crystals

The usual technique for experimentally investigating the transport processes taking place in the condenser-reservoir section of the heat pipe is to measure the axial surface temperature distribution along the outside of the pipe. It is assumed that the thermal resistance through the wick and the pipe wall is small enough that the surface temperature gives an accurate representation of the temperature of the working fluid vapor and noncondensable gas combination. It is also assumed that the working fluid is always at saturation conditions. The surface temperature is therefore assumed to give the local axial vapor saturation temperature and hence the saturation pressure. This saturation pressure corresponds to the partial pressure of working fluid vapor and is therefore representative of the local axial concentration of working fluid vapor. The use of thermocouples placed on a single axial line along the heat pipe tacitly assumes that the temperature and hence the concentration distributions are nearly one dimensional and vary only with the axial coordinate.

To be able to measure any deviation from one dimensional behavior the outside surface of both pipes was coated with a mixture of microencapsulated cholesteric liquid crystals. Cholesteric liquid crystals are formed from esters of cholesterol. These liquid crystals will exhibit all the colors of the visible spectrum as they are heated through their "event temperature range". Both the location on the temperature scale of the

event temperature and the width of the temperature range of the liquid crystals can be controlled by the proper formulation. An excellent comprehensive review of the applications of liquid crystals to heat transfer and temperature measurement problems can be found in the recent work of Cooper, et al. [16]. The useful life of raw liquid crystals has been greatly extended by a process of microencapsulation. In this process, the crystals are coated with gelatin in a polyvinyl alcohol binder. This results in the formation of small spheres of the order of 30 microns in diameter. In this form the liquid crystals are much better able to withstand the deleterious effects of ultraviolet light and other environmental factors. The liquid crystals used in these experiments were in the form of a water based slurry. Three separate liquid crystals designated R-41, R-49, and R-56 were used. The R in the designation indicates that the width of the event temperature range is "regular", i.e. on the order of 3°C from the onset of red to the fading of blue. The number in the designation indicates the temperature at which the colors begin to appear, e.g. R-49 begins to show at red at about 49°C. Since the liquid crystals are viewed by reflected light, it is necessary to provide a black background against which to view them.

Before applying the liquid crystals, both heat pipes were painted with a flat black enamel paint. Equal parts of the three liquid crystals (R-41, R-49, and R-56) were then mixed together. Several coats of this mixture were then applied to the 2.5 cm and 5.0 cm diameter heat pipes. Each coat was allowed to dry before applying the next. The 1.6 cm diameter heat pipe was coated with only the R-49 liquid crystal. During operation, the liquid crystal isotherms on the heat pipes were recorded by measuring the angular position at axial increments of at least 5 cm. of the green color line for a particular isotherm.

3. EXPERIMENTAL PROCEDURE

The filling procedure for each heat pipe consisted of first evacuating the heat pipe to a pressure of 10 microns of mercury by means of a vacuum pump. The proper amount of methanol or Freon was then added from a graduated bottle by regulating the flow with the bellows seal vacuum valve. This process always introduced a small amount of extraneous air. To eliminate the air sufficient power was applied to the heat pipe to raise the pressure inside to well above atmospheric. The heat pipe was allowed to come to a steady state and insure that all the air had accumulated at the condenser end. The bleed screw at the condenser end was then opened, and the unwanted air was allowed to escape. The bleed screw was then closed. This procedure was repeated until the internal pressure at the condenser end was equal to the saturation pressure of methanol corresponding to the measured internal temperature at the condenser end. The partial pressure of air was then zero indicating all the air has been eliminated. The heat pipe was then run as a conventional heat pipe to obtain its operating characteristics. The heat pipe was then filled with the noncondensable gas. The procedure for filling the 5 cm. diameter heat pipe with krypton will be outlined; the procedure is similar for the other gases and the other heat pipes. Initially with the pipe operating at 100 watts nominal power input, sufficient krypton was added to increase the pressure in the pipe by 93. kPa (13.5 psi). After the desired data was recorded, the pipe was vented through the bleed screw to remove approximately one third of the krypton by reducing the system pressure approximately 31. kPa (4.5 psi). The same procedure was followed to produce the third krypton load. The amount of gas in the pipe for a particular load was calculated from the pressure and temperature inside the pipe when the pipe was not operating and therefore at ambient temperature.

3.1 Operating Procedure

Each heat pipe was operated with at least three different amounts of each noncondensable gas. The gas loads for each heat pipe are summarized in table II. For each gas load heat pipe No. 1 was operated at power levels of from 10 to 50 watts in 10 watt increments. Heat pipe No. 2 was operated at power levels of from 20 to 50 watts in 15 watt increments. Heat pipe No. 3 was operated at power levels of from 25 to 150 watts in 25 watt increments. At each power setting steady state data was recorded in both the horizontal and vertical positions. The power settings were subsequently corrected by subtracting the losses through the insulation to obtain the actual power to the heat pipe.

Methanol

	Heat Pipe No. 1	Heat Pipe No. 2	Heat Pipe No. 3	
Krypton	0.076 gm	1.59 gm 0.617	Krypton	
	0.186			7.39 gm
	0.527		5.26	
	0.893		2.75	
Helium	0.008 gm	0.124 0.062 0.031	Helium	
	0.017			0.63
	0.026			0.29
			0.18	

Freon

	Heat Pipe No. 1	Heat Pipe No. 2	Heat Pipe No. 3	
Krypton	—	—	Krypton	
	—			—
	—			—
Helium	—	0.142 gm 0.083	Helium	
	—			—
	—			—

TABLE II
Summary of Gas Loads

4. EXPERIMENTAL RESULTS

The results for the largest and smallest diameter heat pipes exhibit the extremes in the effects of gravity on heat pipe operation: from essentially no effect on heat pipe No. 1 (1.6 cm. diameter) to very pronounced effects on heat pipe No. 3 (5 cm. diameter). The results for these two cases are therefore presented first followed by the results for heat pipe No. 2 (2.5 cm. diameter).

4.1 Heat Pipe No. 1

Figures 4 and 5 show the measured surface temperature distribution from the thermocouples on heat pipe No. 1 (1.6 cm. diameter). They are plotted as the measured surface temperature minus the ambient temperature as a function of distance from the beginning of the condenser. These figures show the characteristic temperature distribution of the gas loaded heat pipe. The higher temperature region is indicative of the active condenser, the lower, near ambient temperature region is indicative of the gas-blocked inactive condenser and the intermediate region of changing temperature is indicative of the gas-vapor interface diffusion region.

From Figure 4, with methanol and helium, the temperature profiles in the horizontal and vertical case are of the same shape, but the position has been shifted. The interface region is shifted toward the condenser in the vertical case, as compared to the horizontal. The lighter helium is tending to rise toward the higher condenser. With methanol and krypton, the shape of the profiles is altered somewhat. From Figure 5, a comparison of the horizontal and vertical profiles indicates that the vapor-gas interface region has been broadened in the vertical case, compared to the same power level in the horizontal case. This effect was more pronounced at the lower power levels. When operating in the vertical position the gravitational force causes the heavier krypton to tend to settle toward

the lower evaporator. This tendency is counteracted by the momentum flux of methanol vapor toward the condenser. The vertical operating position with methanol and krypton is a gravitationally unstable situation (heavier krypton above lighter methanol). This instability is borne out by the observation of the liquid crystal isotherm. In the vertical position the isotherm was in constant motion, randomly oscillating about a mean position with a period of the order of several seconds. The liquid crystal isotherm on heat pipe No. 1 was always nearly perpendicular to the axis of the heat pipe. This seems to indicate that the heat and mass transport processes within a heat pipe of this smaller diameter are nearly one-dimensional.

4.2 Heat Pipe No. 3

Figures 6 and 7 show the surface temperature profiles on heat pipe No. 3. These results at first seem anomalous. In Figure 6, with methanol and helium the vertical temperature profile is consistent with what would be expected for a gas loaded heat pipe. The horizontal profile on the other hand is not. In the horizontal case, the pipe appears to have a temperature distribution which is continuously decreasing, indicating no clear regions of active and inactive condenser. In Figure 7 with methanol and krypton, both the horizontal and vertical cases have this indistinct temperature profile with no clear indication of a vapor-gas interface region. In this case, the liquid crystal isotherms are invaluable in interpreting the temperature distributions.

Figures 8 through 19 are plots of the measured liquid crystal isotherms on heat pipe No. 3. The figures shown are plane projections of one side of the heat pipe. Results for all krypton loads and all helium loads for both the horizontal and vertical positions are shown. Figures 8, 9 and 10 are for two different amounts of krypton with the heat pipe in the horizontal

position. From these figures, it is obvious that stratification of the vapor and noncondensable gas has occurred. The heavier krypton has sunk to the lower portion of the heat pipe and the methanol vapor has risen to occupy the upper portion of the pipe. The isotherms indicate that the krypton is distributed along the full length of the condenser and even seems to penetrate into the adiabatic section. This is particularly apparent in Figure 10 for the higher gas load. For both gas loads, as the power is increased, the stratification becomes more pronounced so that in Figure 9, at 94.1 watts the 56°C isotherm is nearly horizontal.

Figures 11, 12 and 13 are similar plots for two different amounts of helium with the pipe operating in the horizontal position. In this case, the helium migrates to the top of the pipe and the methanol vapor settles to the bottom. Although less severe than with krypton, there is still a tendency toward horizontal stratification. As can be seen in Figure 13, at higher helium loads and higher power levels this tendency is increased. In all the horizontal cases, the liquid crystal isotherms indicate that the vapor transport and vapor-gas diffusion processes are highly three dimensional. This explains the seemingly anomalous surface temperature distributions obtained with the thermocouples.

Figures 14 through 19 show the liquid crystal isotherms for the vertical position for both krypton and helium. In the vertical position the transport processes within the heat pipe are more nearly one dimensional with some modification depending on the particular gas. In Figures 14, 15 and 16, it is apparent that the gravitational force acting on the heavier krypton has a tendency to spread out the vapor gas interface region. Indeed for some power levels and krypton loads, it appears to cover the full length of the pipe. It should be pointed out that the isotherms for the

krypton loaded pipe in the vertical position were in constant motion indicative of the gravitationally unstable nature of this case.

The isotherms for the helium loads in the vertical position are shown in Figures 17, 18 and 19. In this case, gravity is aiding the methanol vapor momentum flux in separating the gas and vapor. The isotherms are very closely spaced; only their location is shifted as the power or helium load is changed. The behavior in the helium/vertical case is in agreement with the usual assumptions for gas-loaded heat pipes.

4.3 Heat Pipe No. 2

Heat pipe No. 2 (2.5 cm. diameter) was run using methanol as the working fluid with either krypton or helium as the noncondensable gas. Additionally, this pipe was also run using FREON - 113 as the working fluid and helium as the non-condensable gas. The combination of Freon with a molecular weight of 187.4 and helium with a molecular weight of 4 gave the largest difference in molecular weights between working fluid and non-condensable gas. It should be pointed out that no change in wick structure was undertaken to accommodate the use of Freon as a working fluid.

Figures 20 and 21 show the measured temperature distributions on heat pipe No. 2. From Figure 20, with methanol and helium the differences between the horizontal and vertical orientation are readily apparent, although not as pronounced as in Figure 6 for heat pipe No. 3 (5 cm. diameter). With methanol and krypton the temperature distributions are as shown in Figure 21. Here, there appears to be no difference between the horizontal and vertical orientation. Again, by examining the isotherms obtained from the liquid crystals, as shown in Figures 22 to 31, it is apparent that the temperature distribution obtained from thermocouples placed on a single line along the axis of the pipe can be somewhat

misleading. Although these liquid crystal isotherms do not indicate the severe degree of stratification in the horizontal position that occurs with heat pipe No. 3 (5 cm. diameter), they do show a definite distortion of the temperature distribution. From Figures 22 to 25, for methanol and krypton, the effect of gravity seems to be to distort the isotherms because of the tendency of the working fluid and non-condensable gas to stratify horizontally. For methanol and helium, Figures 26 to 31, the tendency to horizontal stratification is less pronounced. The difference between the horizontal and vertical orientation seem to be a difference in the width of the diffusion interface region between the working fluid and the noncondensable gas. This is apparent from both the thermocouple data (Fig. 20) and the liquid crystal data. The results for heat pipe No. 2, as might be expected, lie between those for the larger and smaller heat pipes.

A few experiments were conducted with the 2.5 cm. diameter heat pipe using Freon-113 as the working fluid and helium as the non-condensable gas. Figure 32 shows the axial temperature distributions obtained with the thermocouples. Here, also the differences between the horizontal and vertical positions are quite obvious. The liquid crystal data shown in Figures 33 to 36 exhibit the same qualitative features as were found in the methanol-helium data. In the horizontal position, with Freon as the working fluid, the liquid crystal isotherms exhibited a slight degree of assymetry. It was felt that this assymetry was probably due to non-uniformities in the wick structure which could have caused local variations in the wick thermal resistance.

5. CONCLUSIONS

It has been demonstrated that orientation in the gravitational field can have a serious effect on the operation of gas-loaded heat pipes in which the working fluid and noncondensable gas are of significantly different molecular weights. For the smallest diameter pipe (1.6 cm.) the effect of gravity is to distort and displace the vapor-gas interface region while not seriously affecting the basically one-dimensional nature of the transport processes within the pipe.

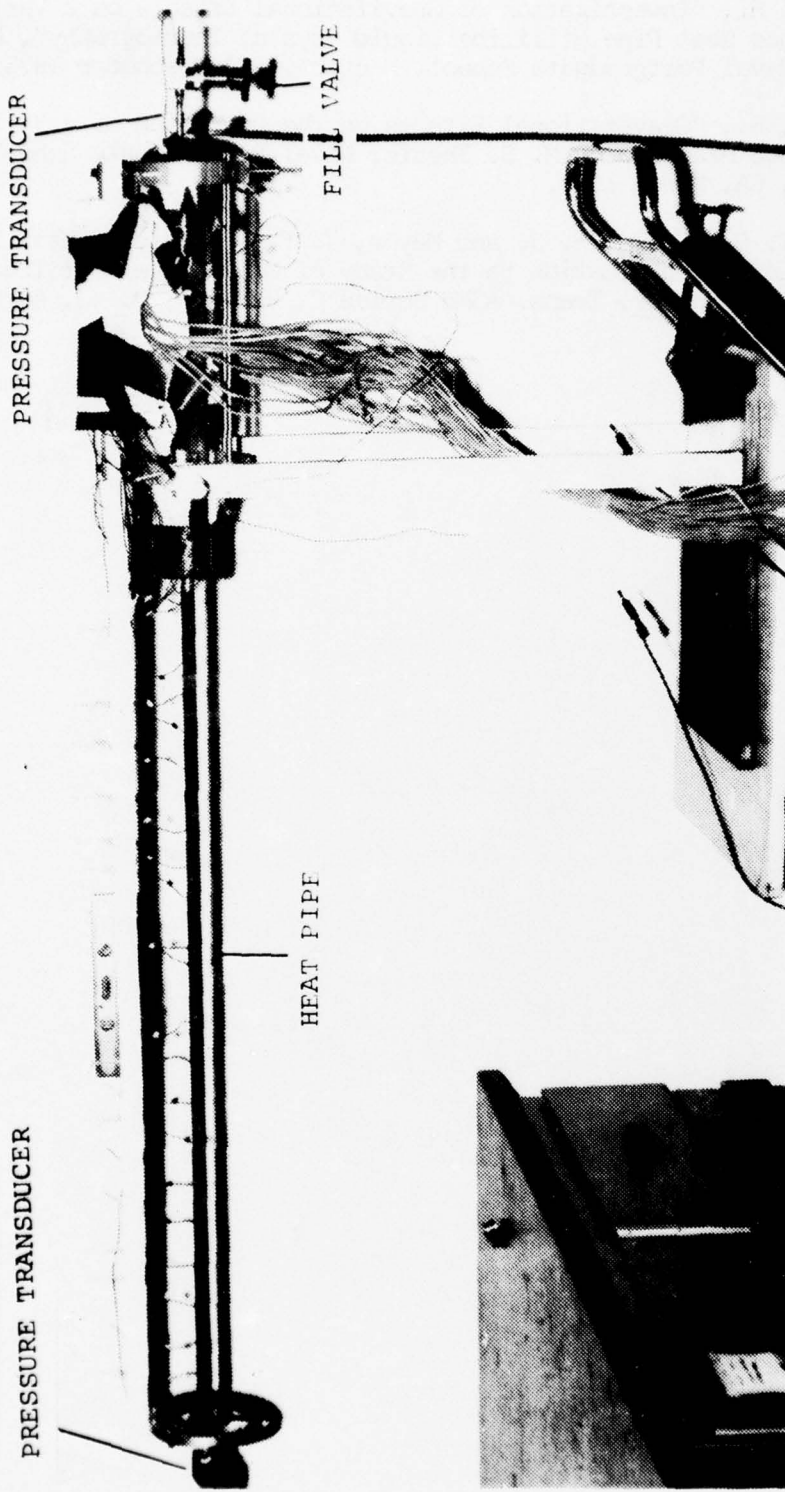
For the largest diameter pipe (5 cm.) the effects of gravity are more profound. In the horizontal operating position stratification of the working fluid vapor and noncondensable gas occurs. The vapor and gas separate into horizontal layers. In this case, the transport processes inside the pipe are highly three dimensional. In the vertical position with the large diameter pipe, gravity induces a distortion of the vapor-gas interface region which is more severe than for the smaller pipe.

No attempt has been made to determine what role other factors such as capillary pumping or wall conduction might play in the observed phenomena. It has been assumed that the large molecular weight differences were the dominant factor.

REFERENCES

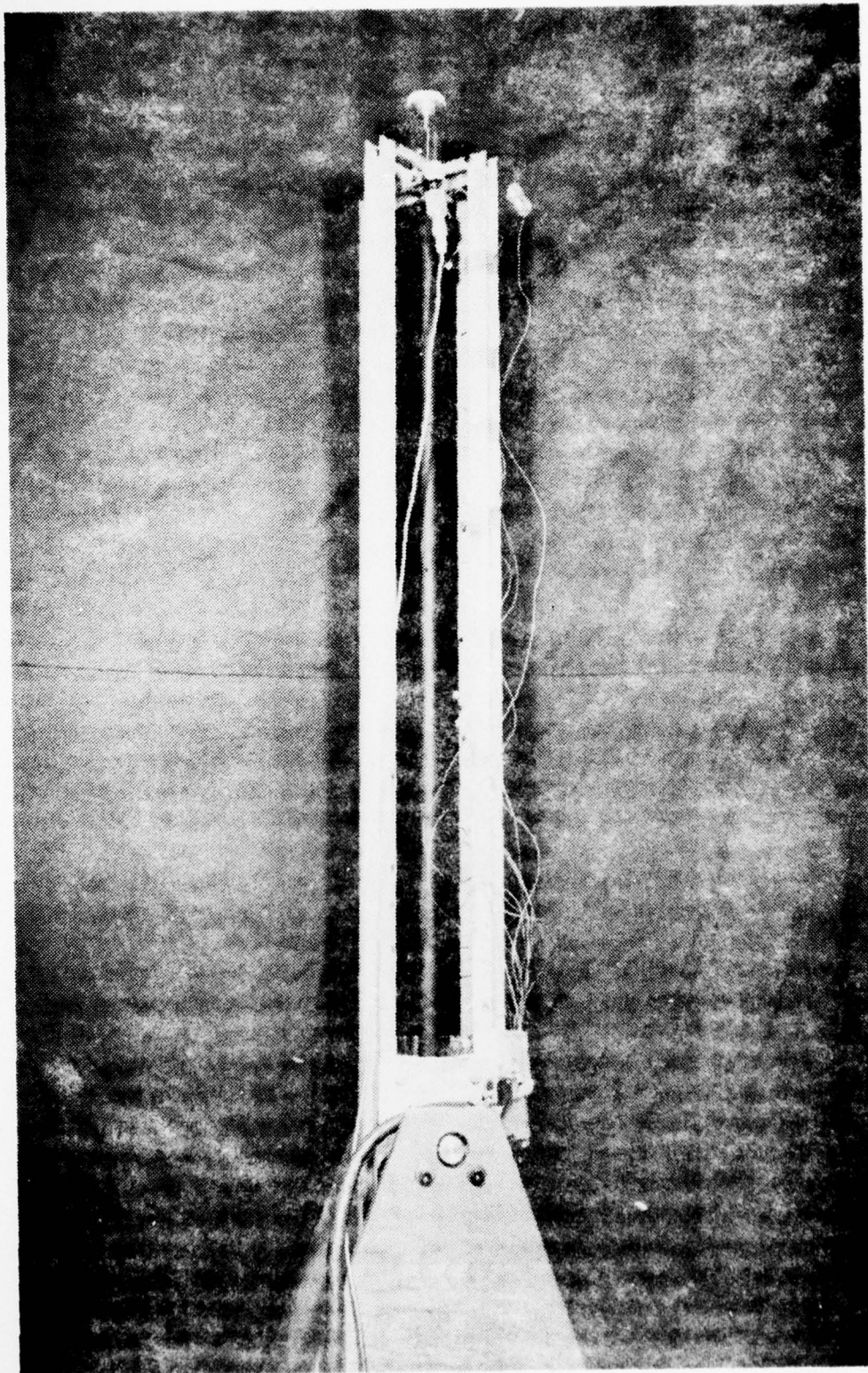
1. Marcus, B. D., "Theory and Design of Variable Conductance Heat Pipes: Control Techniques," NASA CR-2018, April 1972.
2. Marcus, B. D. and Fleischman, G. L., "Steady-State and Transient Performance of Hot Reservoir Gas-Controlled Heat Pipes", ASME Paper No. 70-HT/SpT-11, 1970.
3. Edwards, D. K., Fleischman, G. L. and Marcus, B. D., "Theory and Design of Variable Conductance Heat Pipes: Steady State and Transient Performance", Research Report No. 3, NASA CR-114530, December 1972.
4. Marcus, B. D., Edwards, D. K. and Anderson, W. T., "Variable Conductance Heat Pipe Technology", Research Report No. 4, TRW Report No. 13111-6055-RU-00, December 1973.
5. Kirkpatrick, J. R. and Marcus, B. D., "A Variable Conductance Heat Pipe Flight Experiment", Fundamentals of Spacecraft Thermal Design, Prog. Astronautics and Aeronautics, Vol. 29, John W. Lucas, Ed., p. 505, 1972.
6. Groll, M. and Kirkpatrick, J. P., "Heat Pipes for Spacecraft Temperature Control - An Assessment of the State of the Art", Proceedings of the Second International Heat Pipe Conference, Bologna, Italy, March/April 1976.
7. Anderson, W. T., et. al., "Variable Conductance Heat Pipe Technology - Final Research Report", NASA CR-114750, March 1974.
8. Kirkpatrick, J. P. and Marcus, B. D., "A Variable Conductance Heat Pipe/Radiator for the Lunar Surface Magnetometer", Thermal Control and Radiation, Prog. Astronautics and Aeronautics, Vol. 31, Chang-Lin Tien, Ed., p. 83, 1973.
9. Bienert, W., "Heat Pipes for Temperature Control," 4th IECEC, September 1969, p. 1033.
10. Rohani, A. R. and Tien, C. L., "Steady Two-Dimensional Heat and Mass Transfer in the Vapor-Gas Region of a Gas-Loaded Heat Pipe," Journal of Heat Transfer, Trans, ASME Series C, Vol. 95, No. 3, August 1973, pp. 377-382.
11. Edwards, D. K. and Marcus, B. D., "Heat and Mass Transfer in the Vicinity of Vapor-Gas Front in Gas-Loaded Heat Pipe," J. of Heat Transfer, Trans. ASME Series C, Vol. 94, No. 2, May 1972, pp. 155-162.
12. Humphries, W. I., "Investigation of Gravitational Effects on the Performance of a Variable Conductance Heat Pipe," M. S. Thesis, Naval Postgraduate School, Monterey, California, December 1973.
13. Nayden, T. P., "Investigation of a Variable Conductance Heat Pipe", M. S. Thesis, Naval Postgraduate School, Monterey, California, March 1975.

14. Batts, W. H., "Investigation of Gravitational Effects on a Variable Conductance Heat Pipe Utilizing Liquid Crystal Thermography", M. S. Thesis, Naval Postgraduate School, Monterey, CA, December 1975.
15. Owendoff, R., "Gravitational Effects on the Operation of a Variable Conductance Heat Pipe", M. S. Thesis, Naval Postgraduate School, Monterey, CA, March 1977.
16. Cooper, T. E., Field, R. J. and Meyer, J. F., "Liquid Crystal Thermography and Its Application to the Study of Convective Heat Transfer", J. of Heat Transfer, Trans. ASME Series C, Vol. 97, No. 3, August 1975, pp. 442-450.



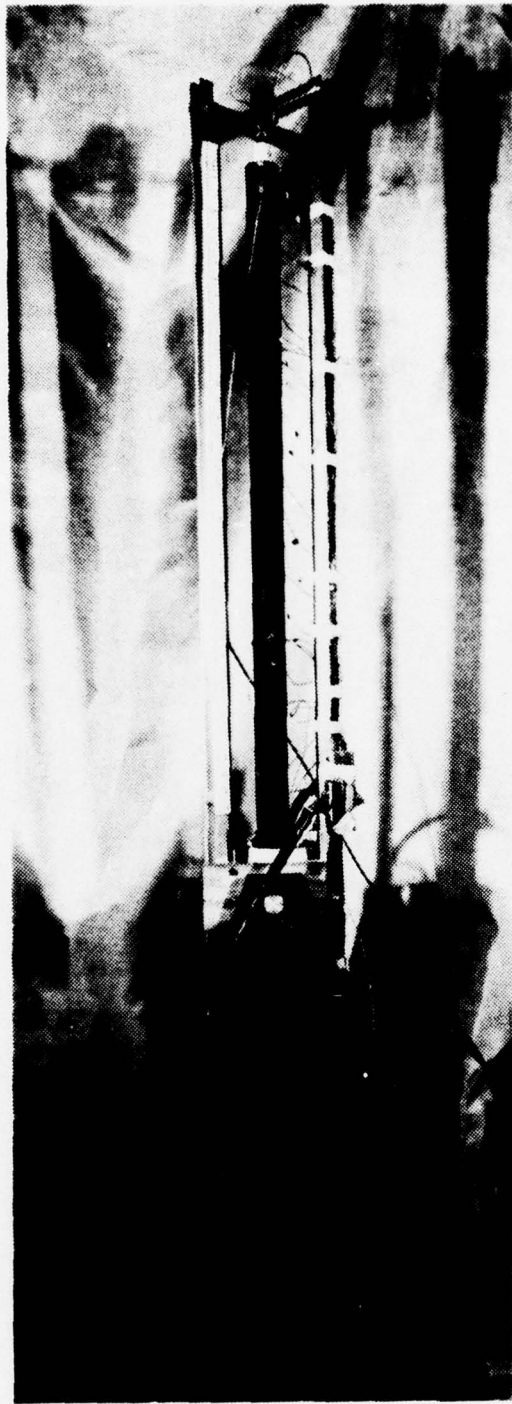
Photograph of Heat Pipe No. 1 (1.6 cm Diameter)

FIGURE 1



Photograph of Heat Pipe No. 2 (2.5 cm Diameter)

FIGURE 2



Photograph of Heat Pipe No. 3 (5 cm. Diameter)

FIGURE 3

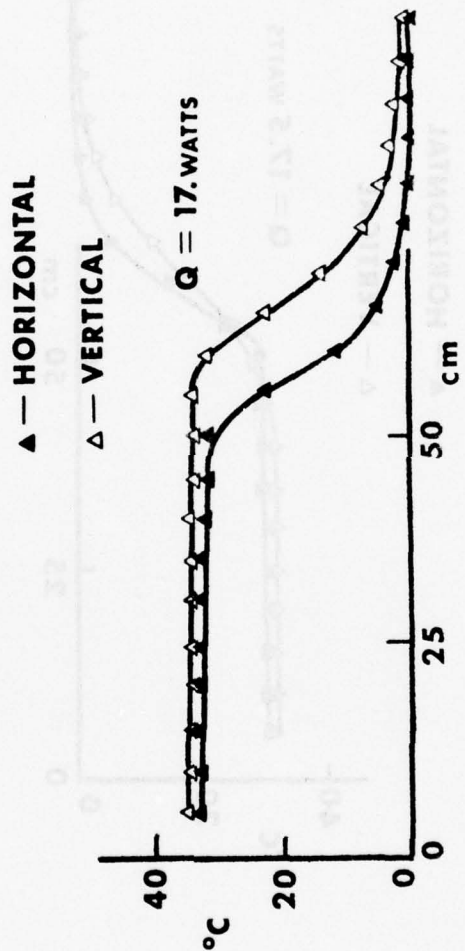


FIGURE 4. Surface minus Ambient Temperature vs. Condenser Length
 Methanol-Helium

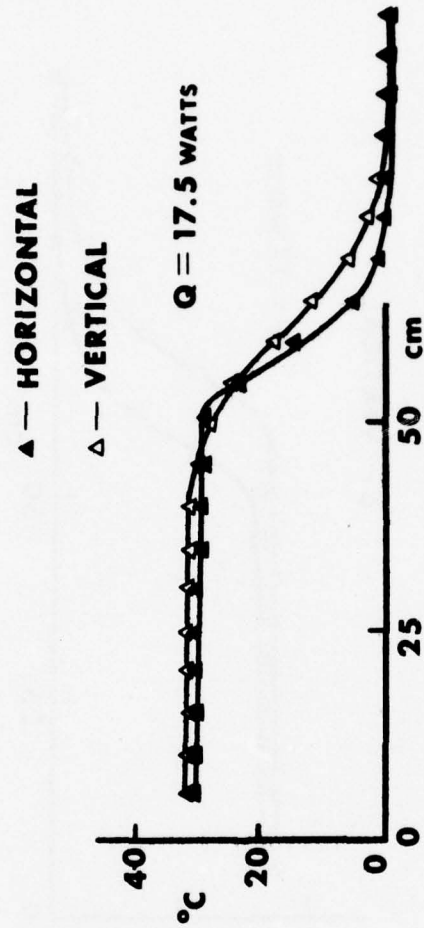


FIGURE 5. Surface minus Ambient Temperature vs. Condenser Length
Methanol-Krypton

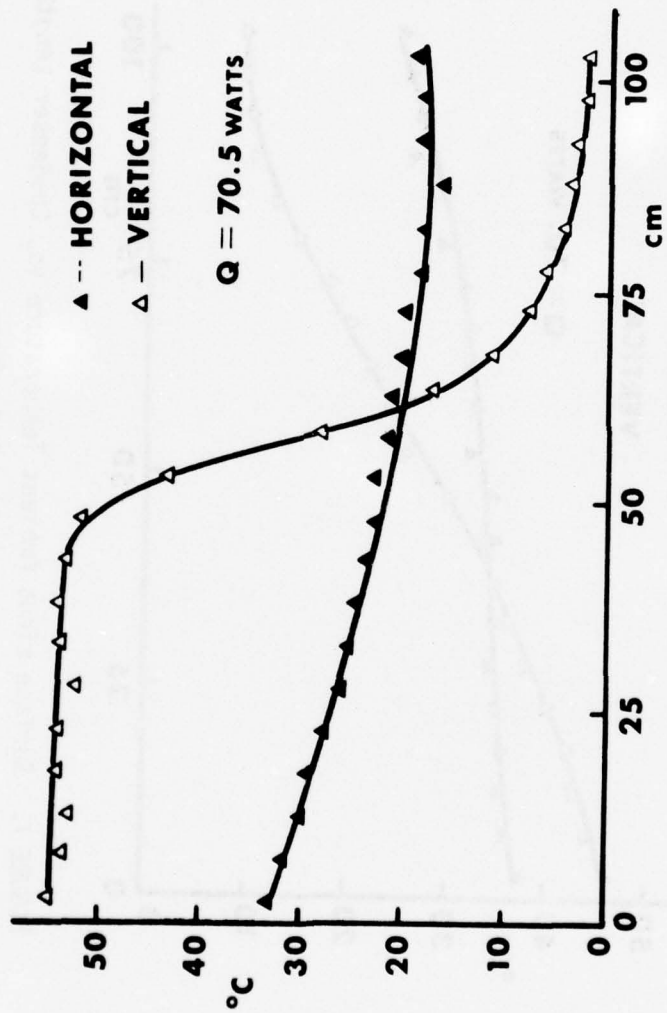


FIGURE 6. Surface minus Ambient Temperature vs. Condenser Length
 Methanol-Helium

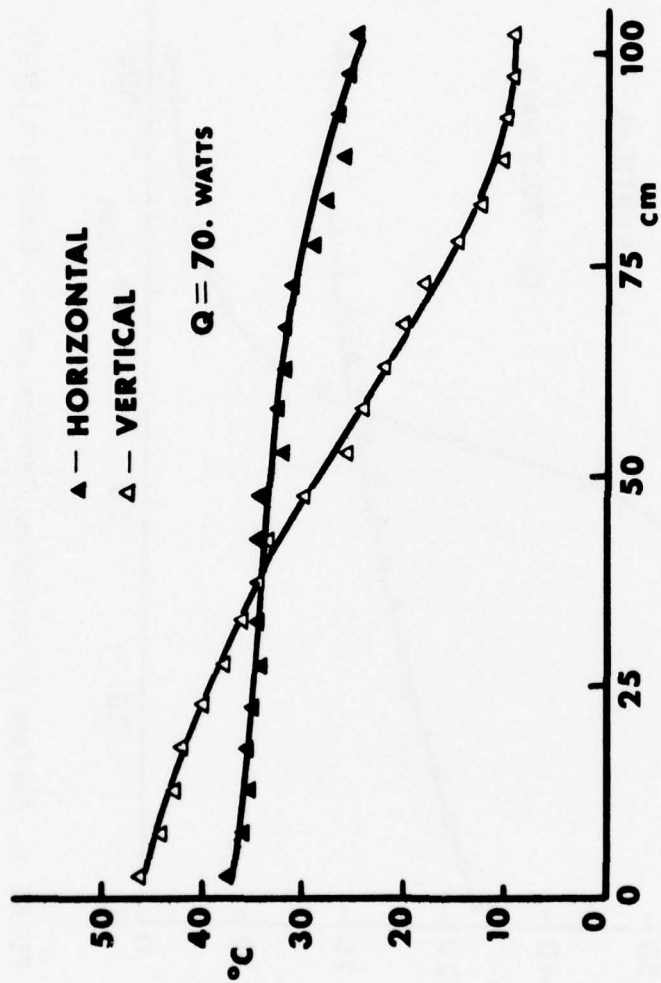


FIGURE 7. Surface minus Ambient Temperature vs. Condenser Length
Methanol-Krypton

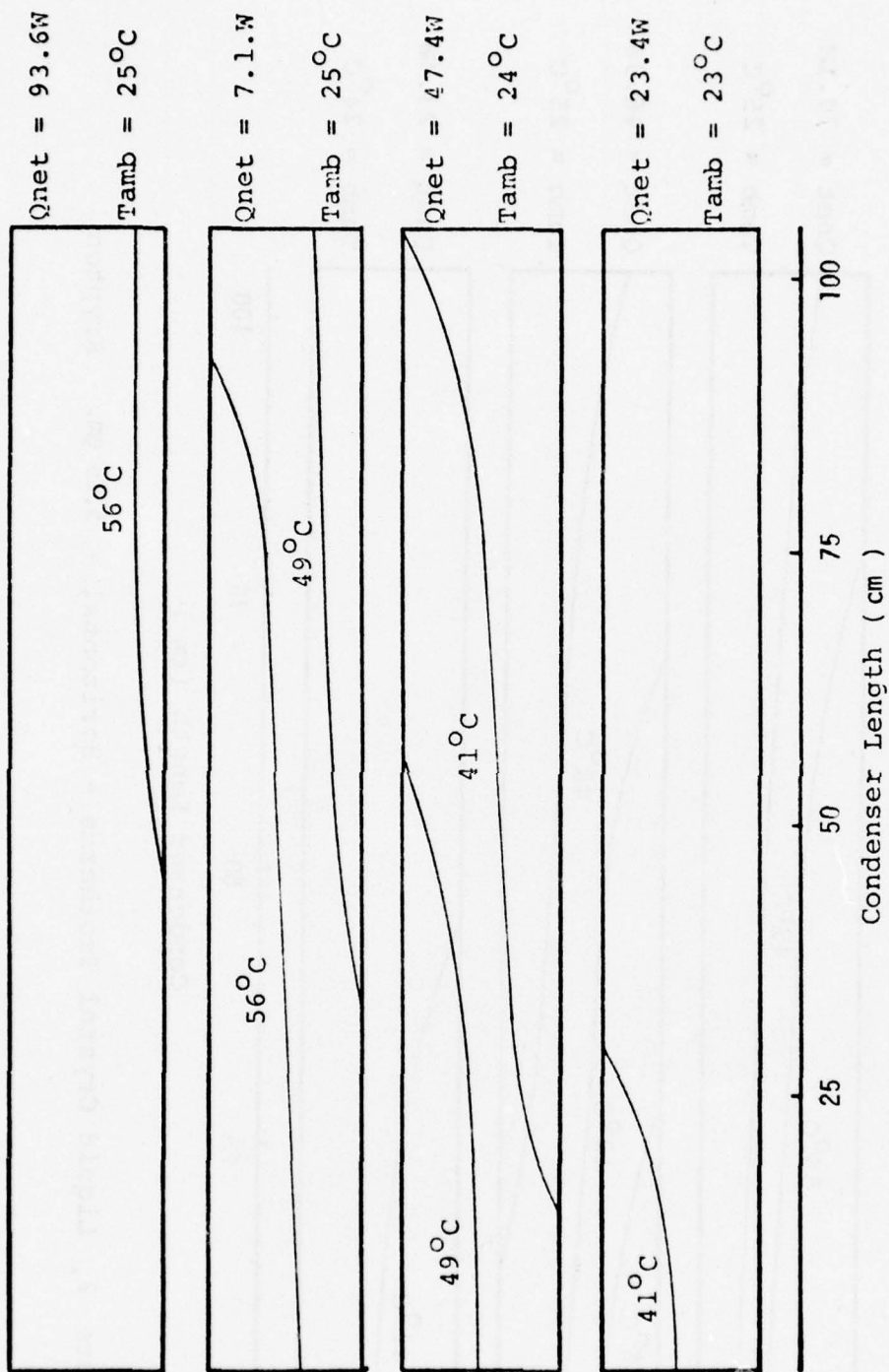


Figure 3. Liquid Crystal Isotherms - Horizontal - 2.75 gm Krypton

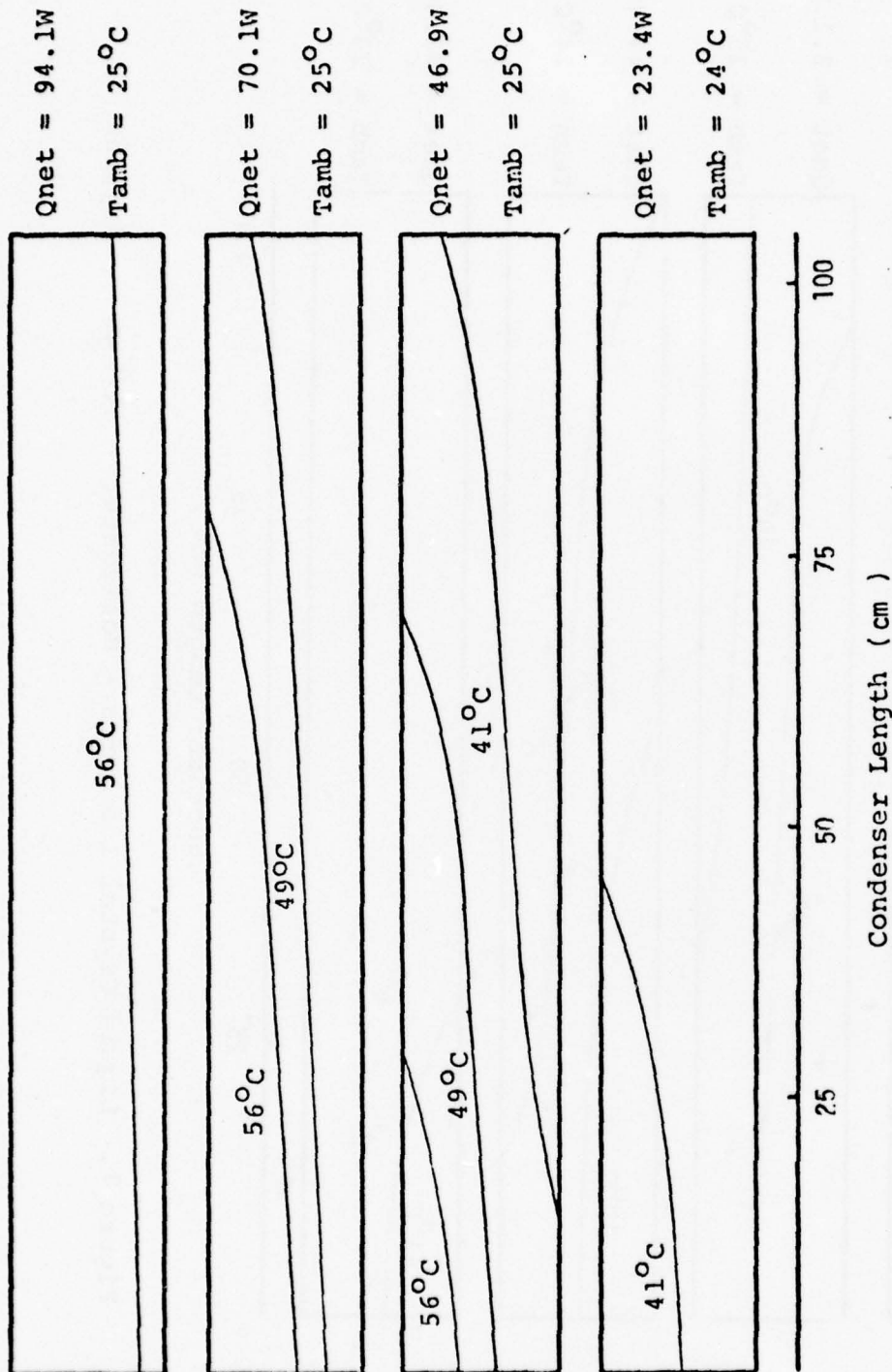


Figure 8. Liquid Crystal Isotherms - Horizontal - 5.26 gm. Krypton

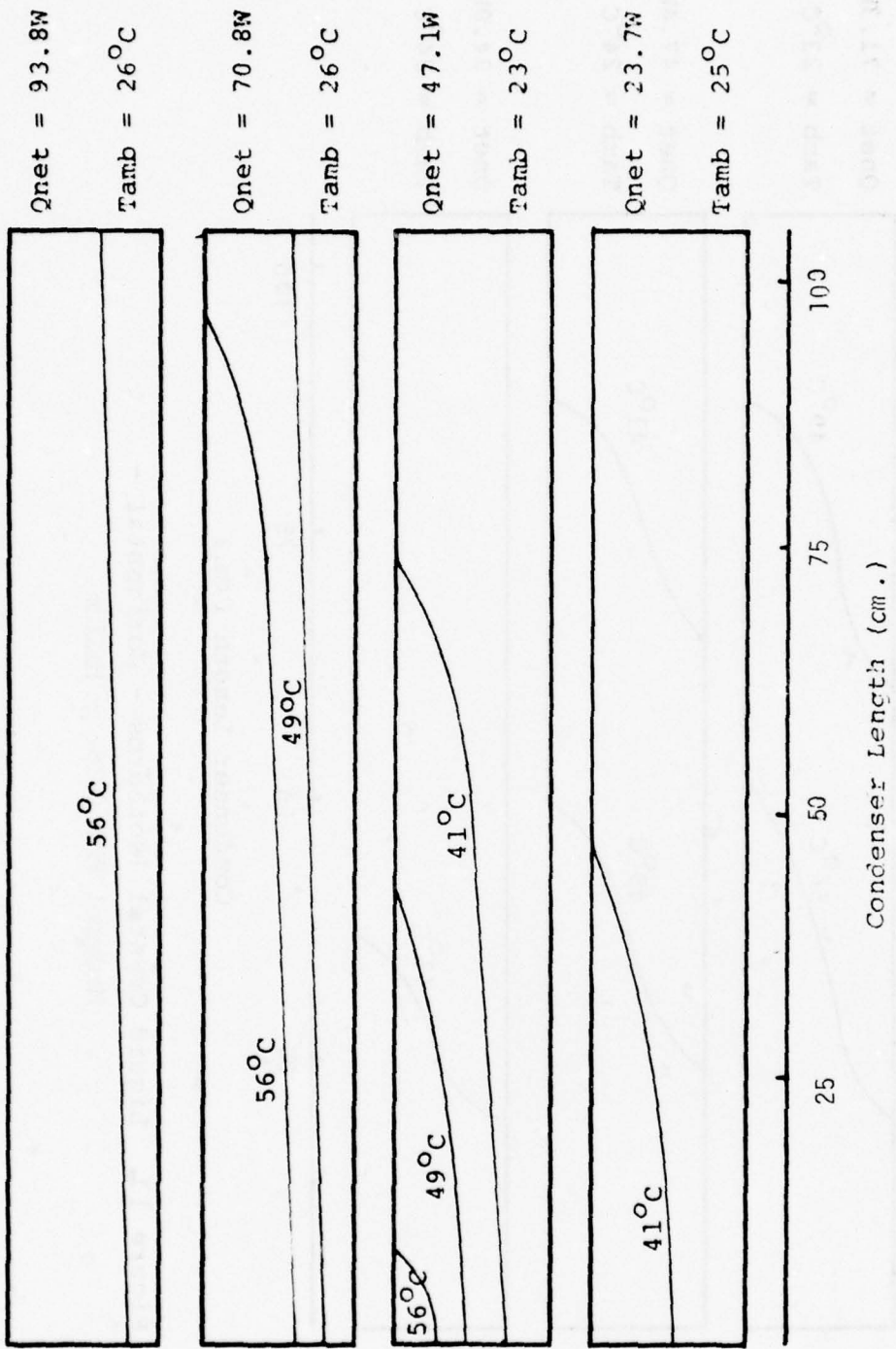


Figure 10. Liquid Crystal Isotherms - Horizontal -
Methanol with 7.39 gm Krypton

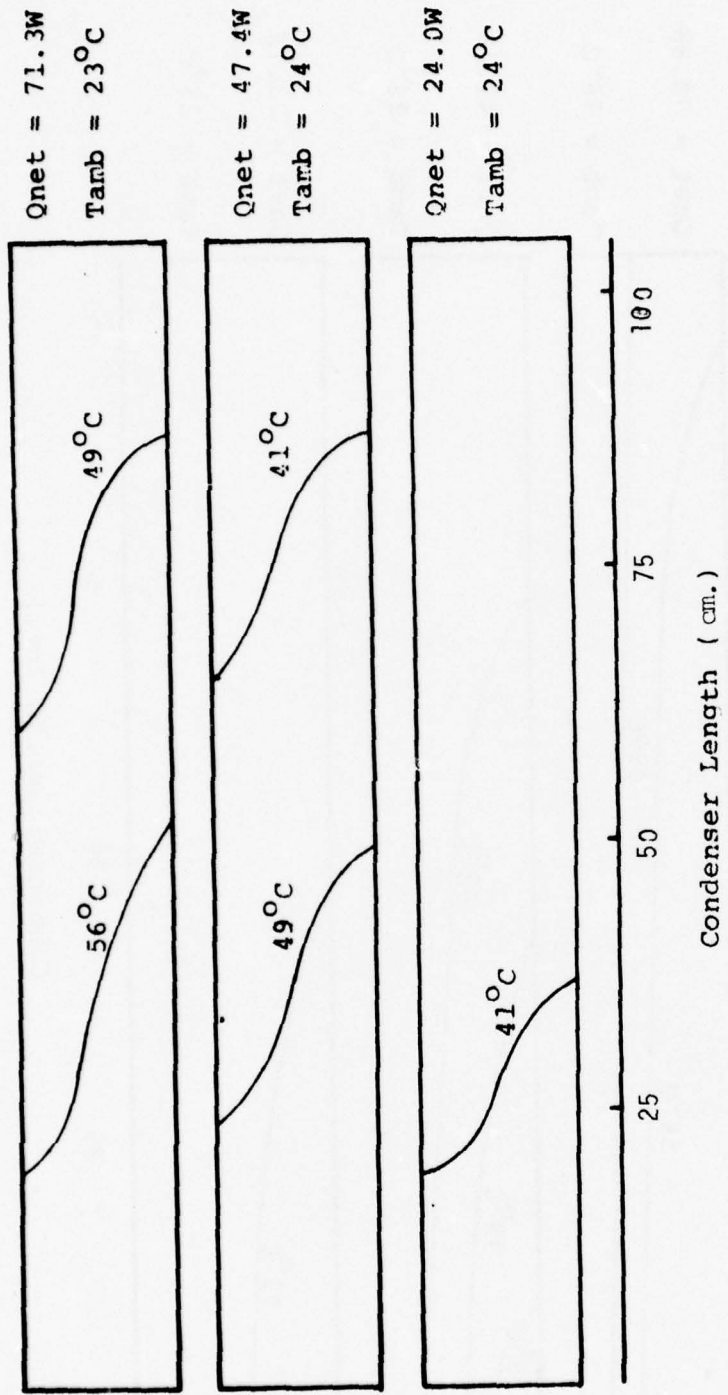


Figure 11. Liquid Crystal Isotherms - Horizontal -
Methanol With 0.182 gm Helium

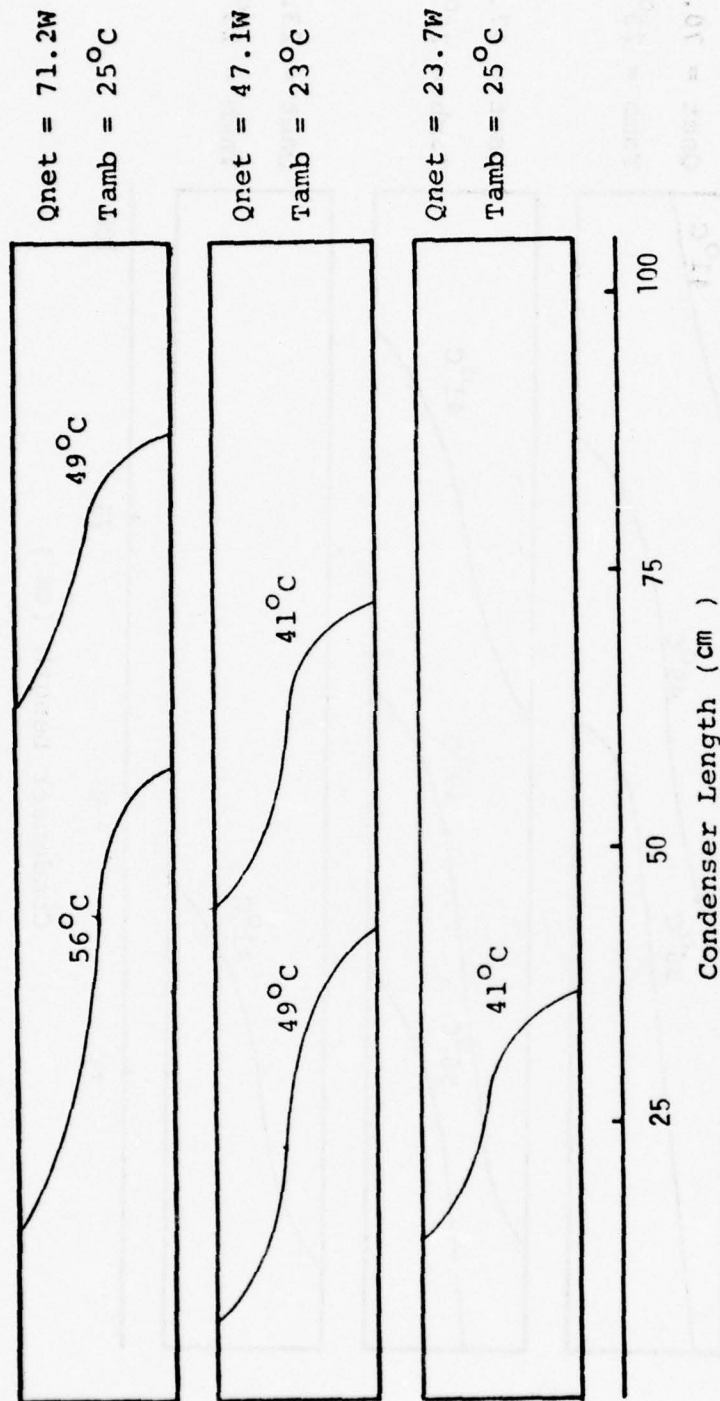


Figure 12. Liquid Crystal Isotherms - Horizontal - 0.29 mm. Helium

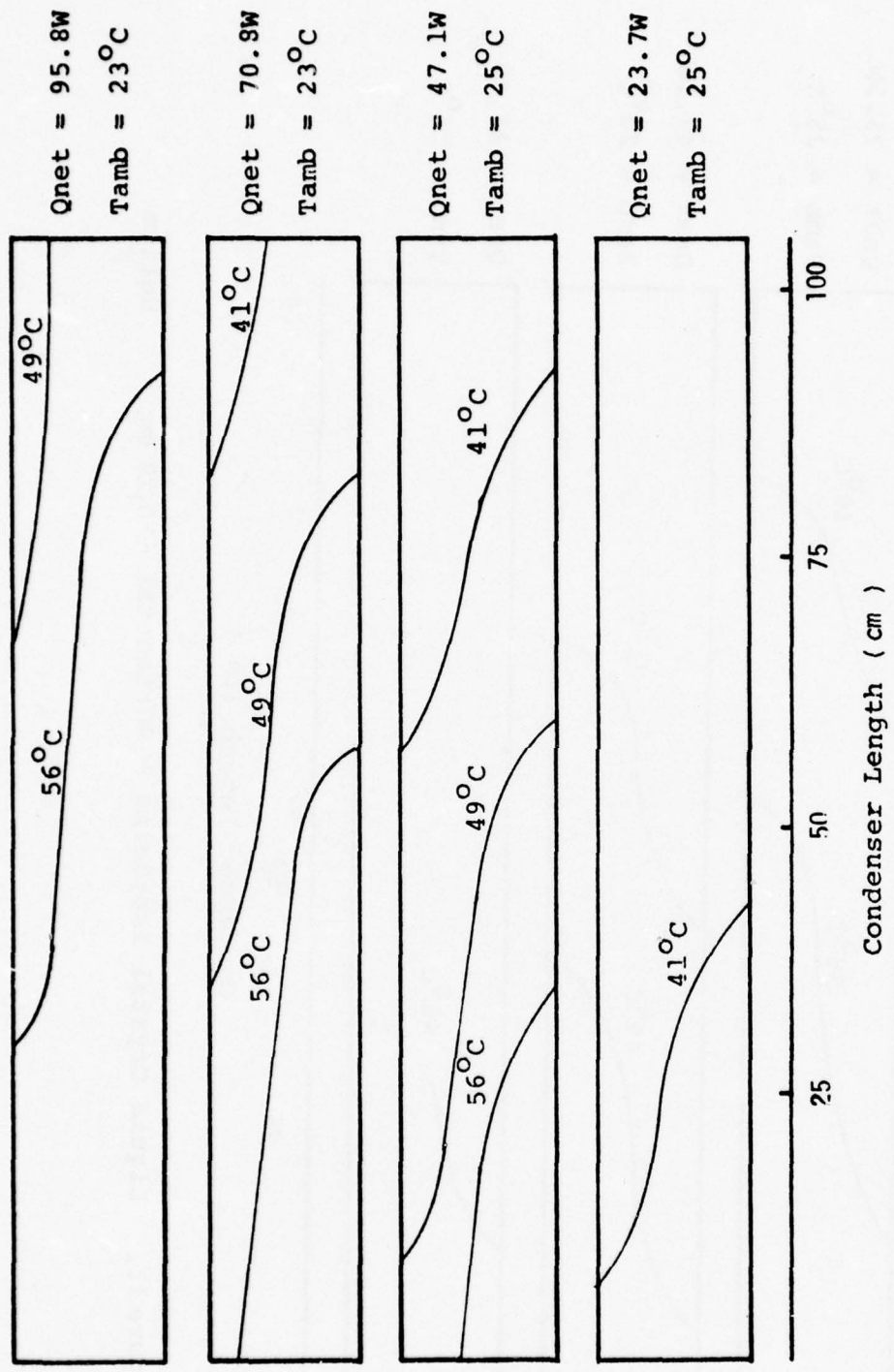


Figure 13. Liquid Crystal Isotherms - Horizontal - 0.63 gm. Helium

Qnet -	22.9W	46.6W	70.2W	94.2W
Tamb -	25°C	26°C	26°C	25°C

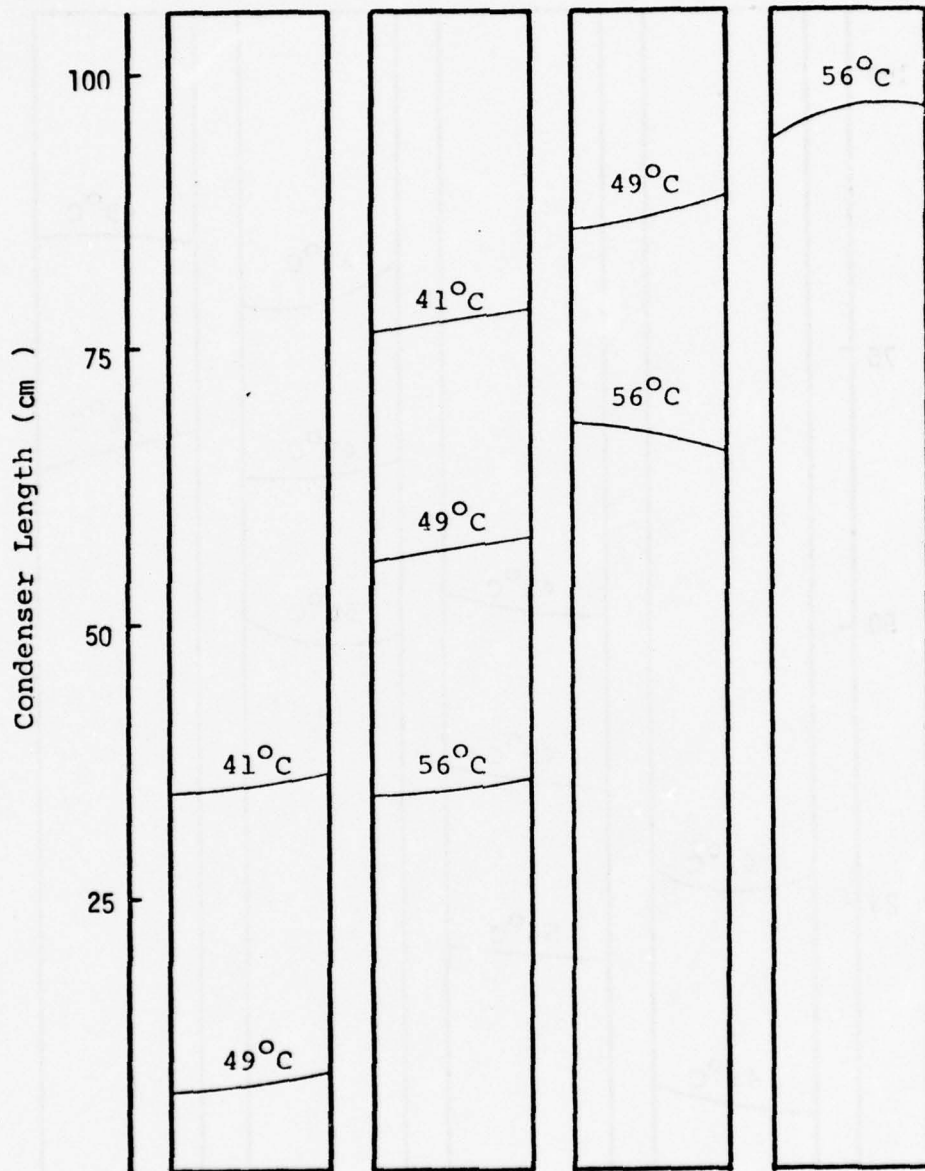


Figure 14. Liquid Crystal Isotherms - Vertical -
2.75 gm. Krypton

Q_{net} -	22.7W	46.4W	70.1W	94.5W
T_{amb} -	25°C	24°C	25°C	25°C

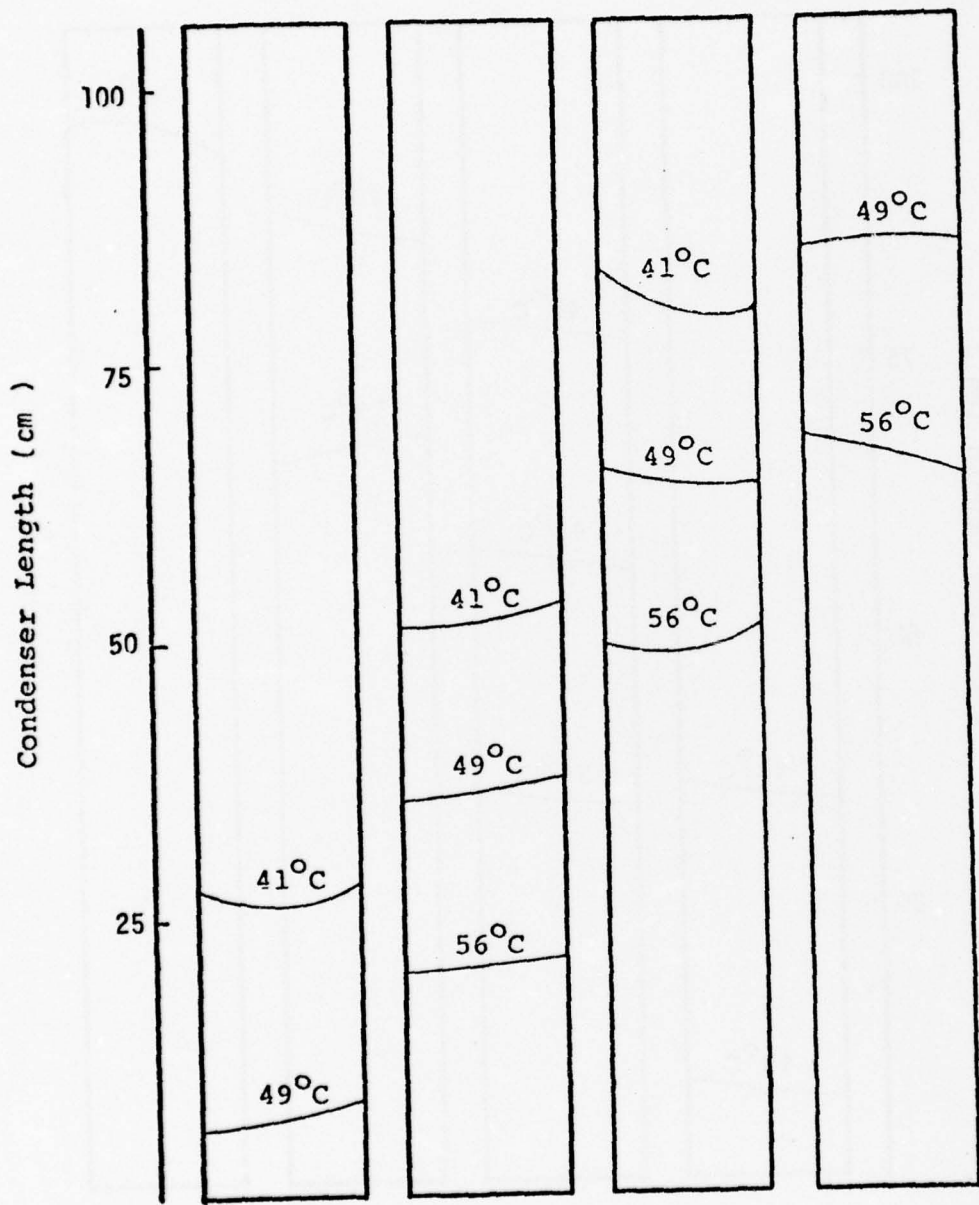


Figure 15 Liquid Crystal Isotherms - Vertical -
5.26 gm. Krypton

Qnet -	22.6W	45.7W	69.8W	94.2W
Tamb -	25°C	25°C	25°C	24°C

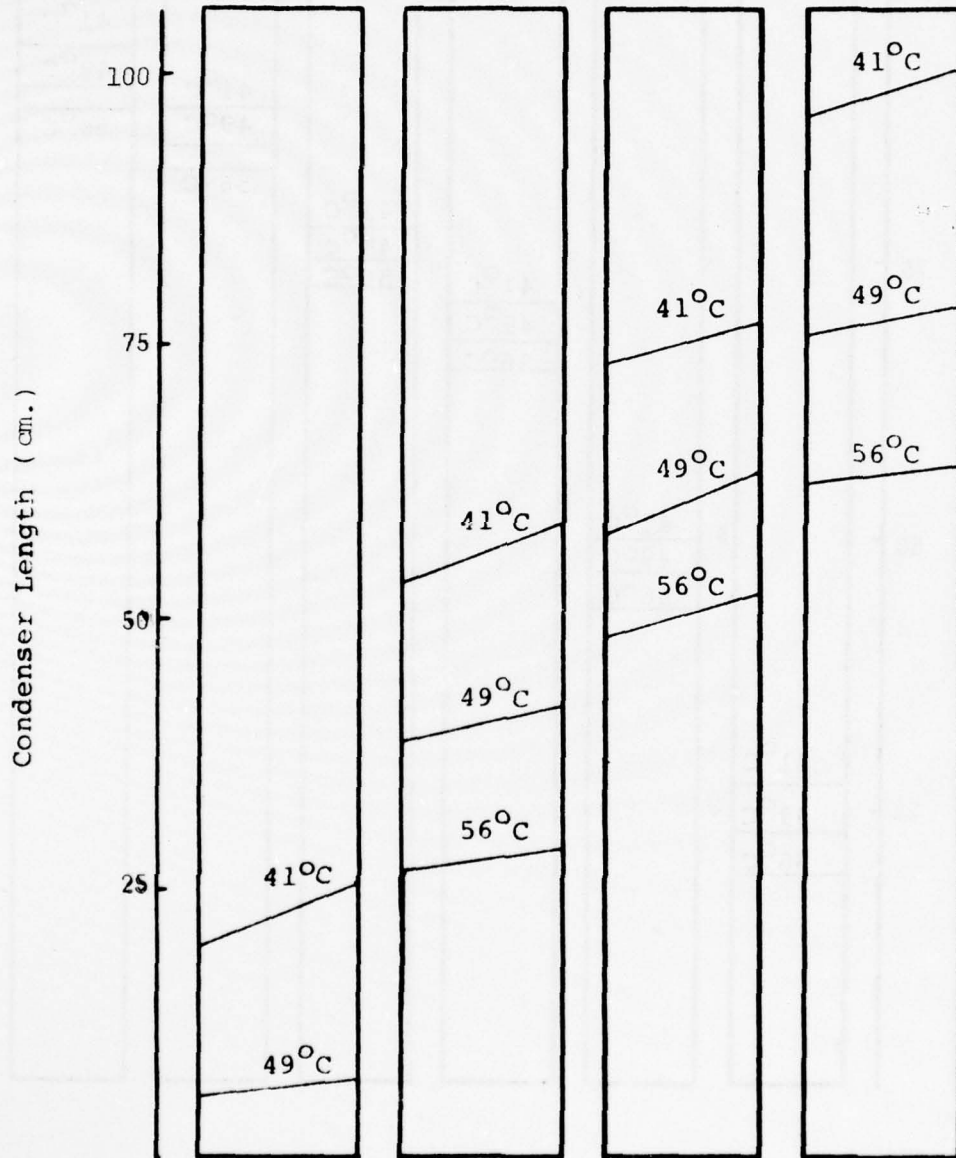


Figure 16. Liquid Crystal Isotherms - Vertical - Methanol With 7.39 gm Krypton

Qnet -	22.9W	46.6W	70.4W	94.4W	118.2W	142.4W
Tamb -	23°C	24°C	25°C	24°C	26°C	26°C

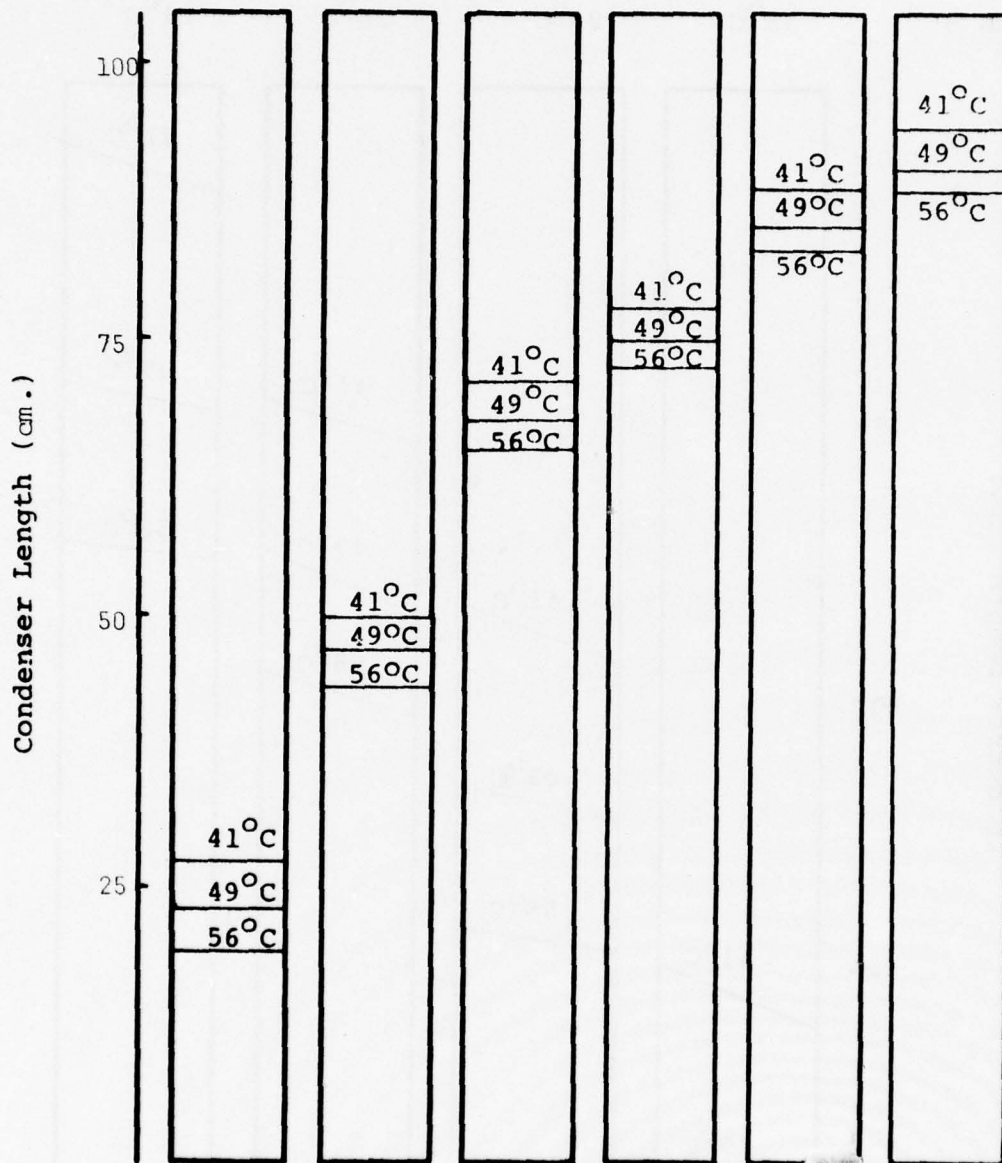


Figure 17. Liquid Crystal Isotherms - Vertical - Methanol With 0.182 gm Helium

Qnet -	22.6W	46.4W	70.0W	94.3W	117.9W	141.8W
Tamb -	24°C	23°C	25°C	25°C	25°C	24°C

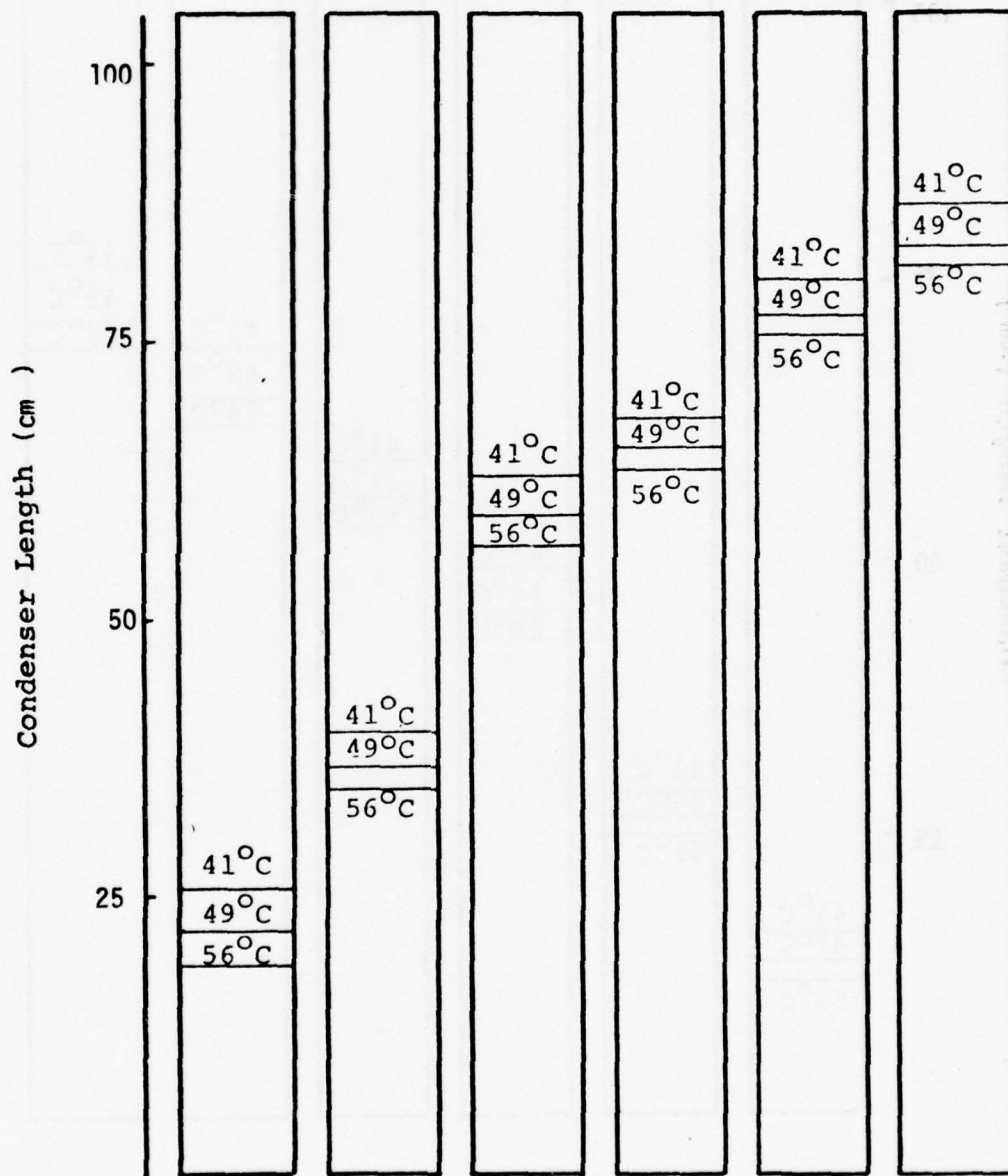


Figure 18. Liquid Crystal Isotherms - Vertical -
0.29 gm. Helium

Q_{net} -	21.3W	45.4W	69.4W	93.7W	117.6W	141.7W
T_{amb} -	24°C	24°C	25°C	24°C	26°C	26°C

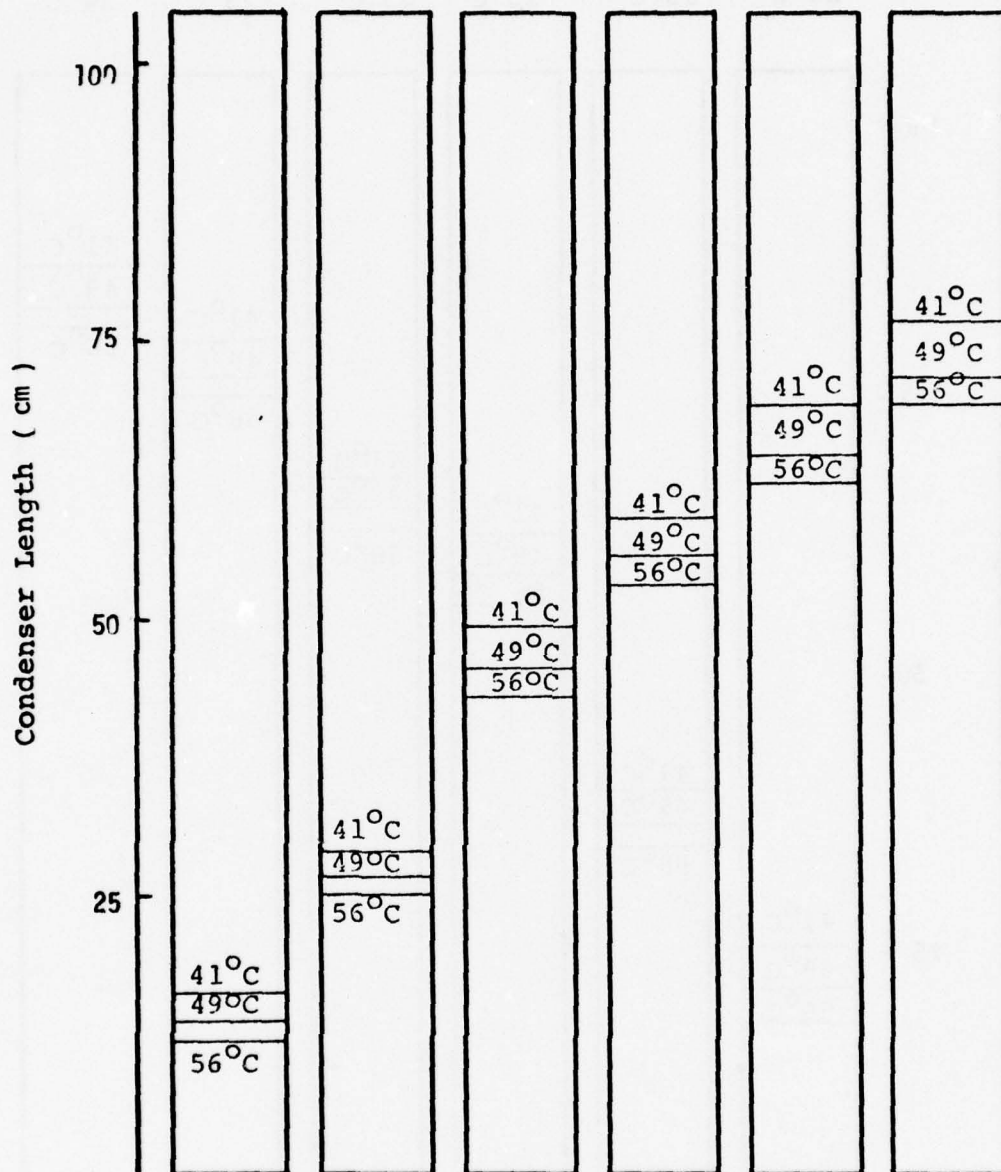


Figure 19. Liquid Crystal Isotherms - Vertical -
0.63 gm. Helium

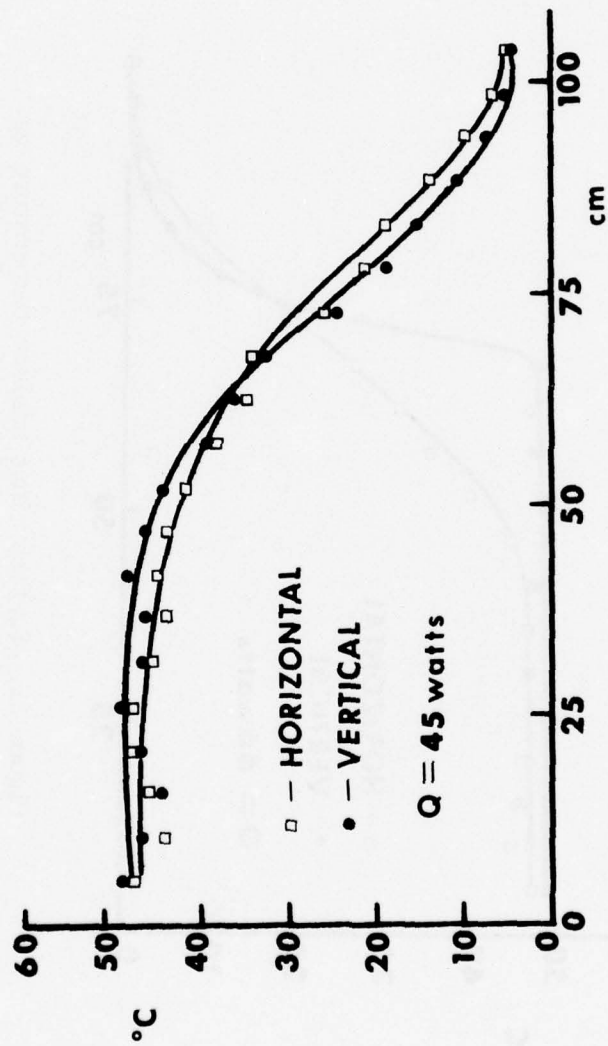


Figure 20. Surface minus ambient temperature vs. Condenser Length; Methanol - Krypton (Heat Pipe No. 2)

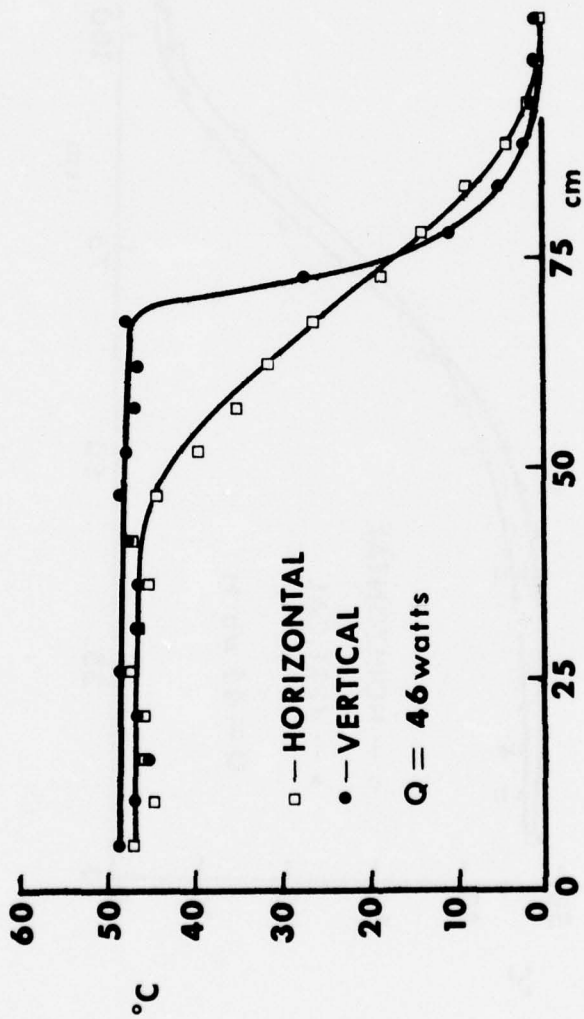
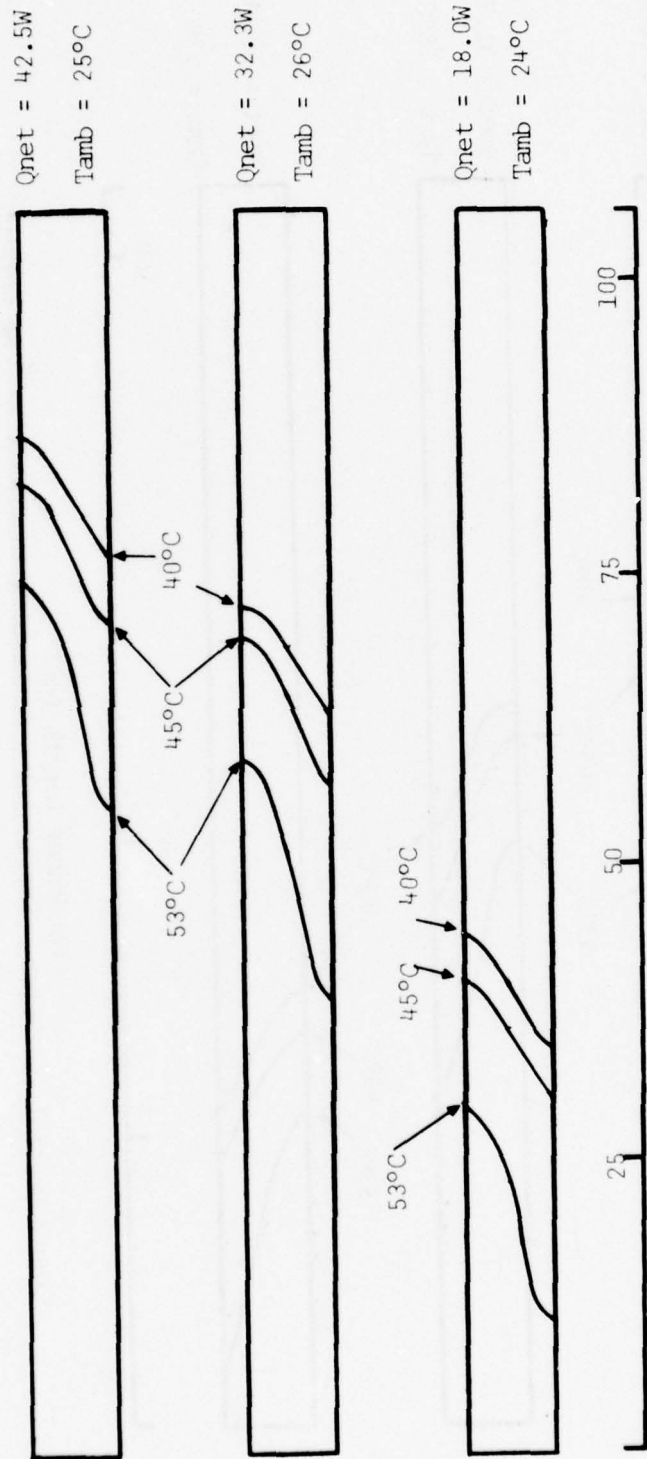
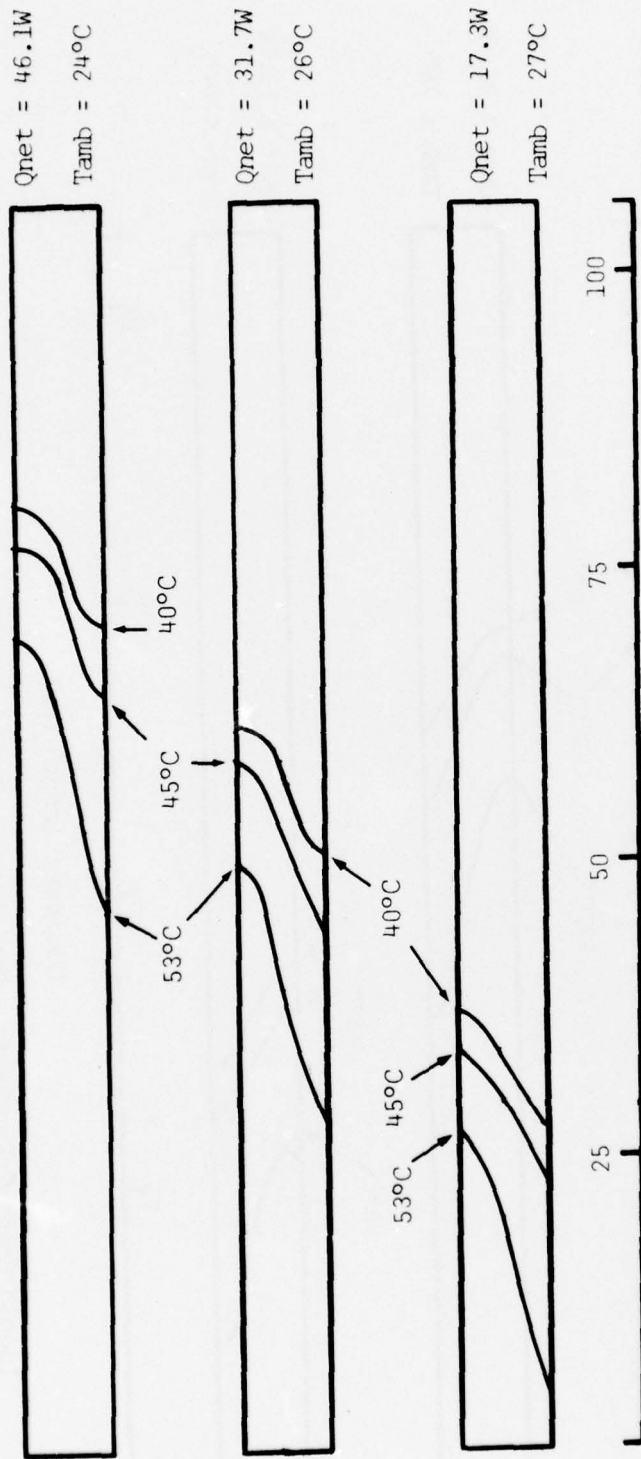


Figure 21. Surface minus ambient temperature vs. Condenser Length; Methanol - Helium (Heat Pipe No. 2)



Liquid Crystal Isotherms - Horizontal - Methanol with 6.17×10^{-4} kg Krypton

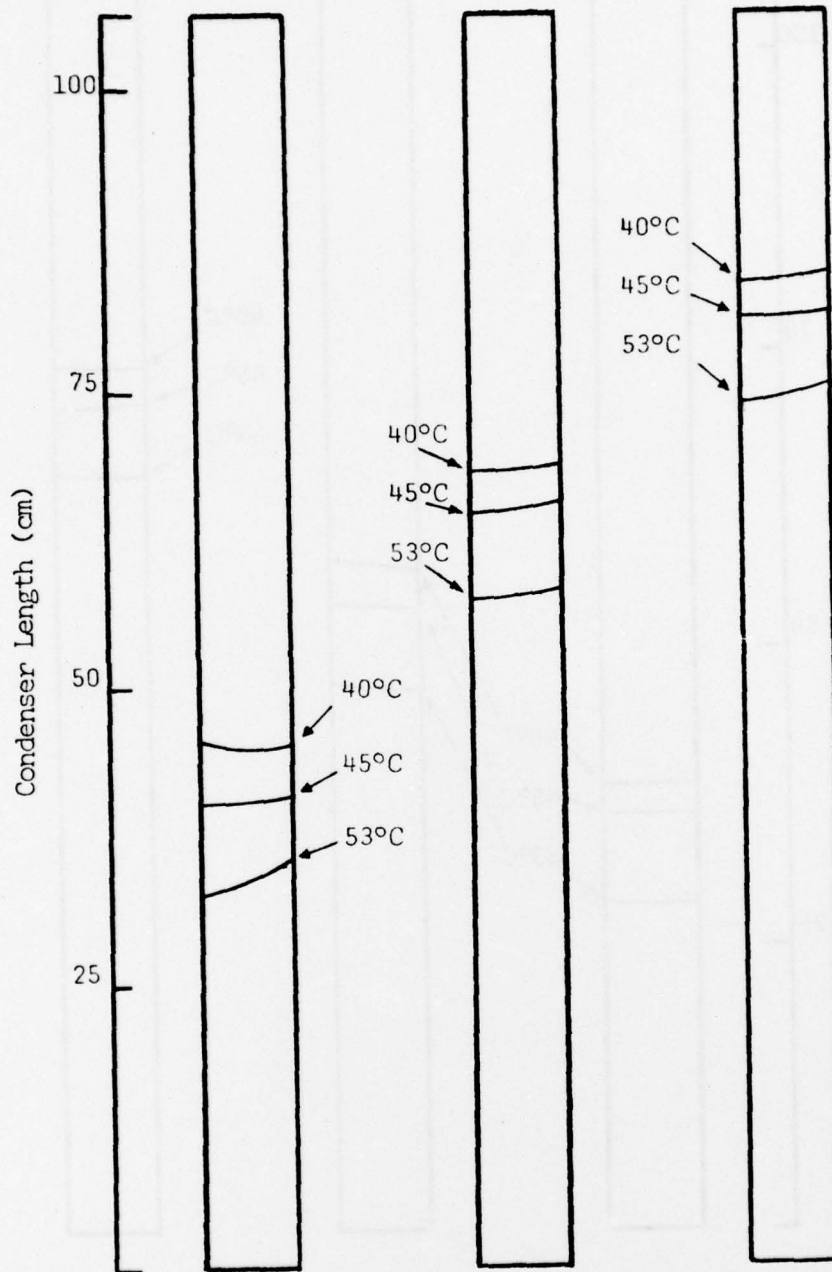
Figure 22



Condenser Length (cm)
 Liquid Crystal Isotherms - Horizontal - Methanol with 1.59×10^{-3} kg Krypton

Figure 23

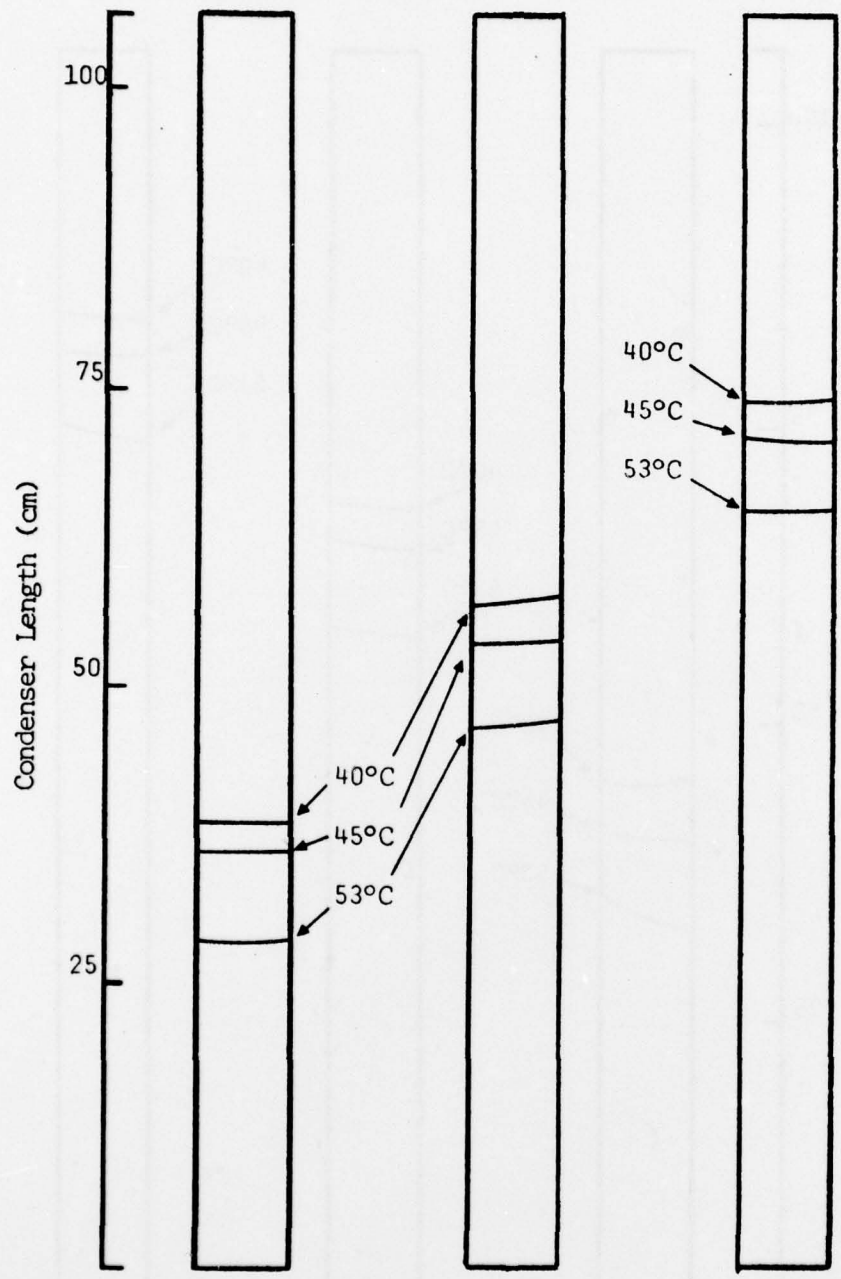
Qnet =	18.2W	32.5W	47.3W
Tamb =	24°C	25°C	27°C



Liquid Crystal Isotherms₄ - Vertical
Methanol with 6.17×10^{-4} kg Krypton

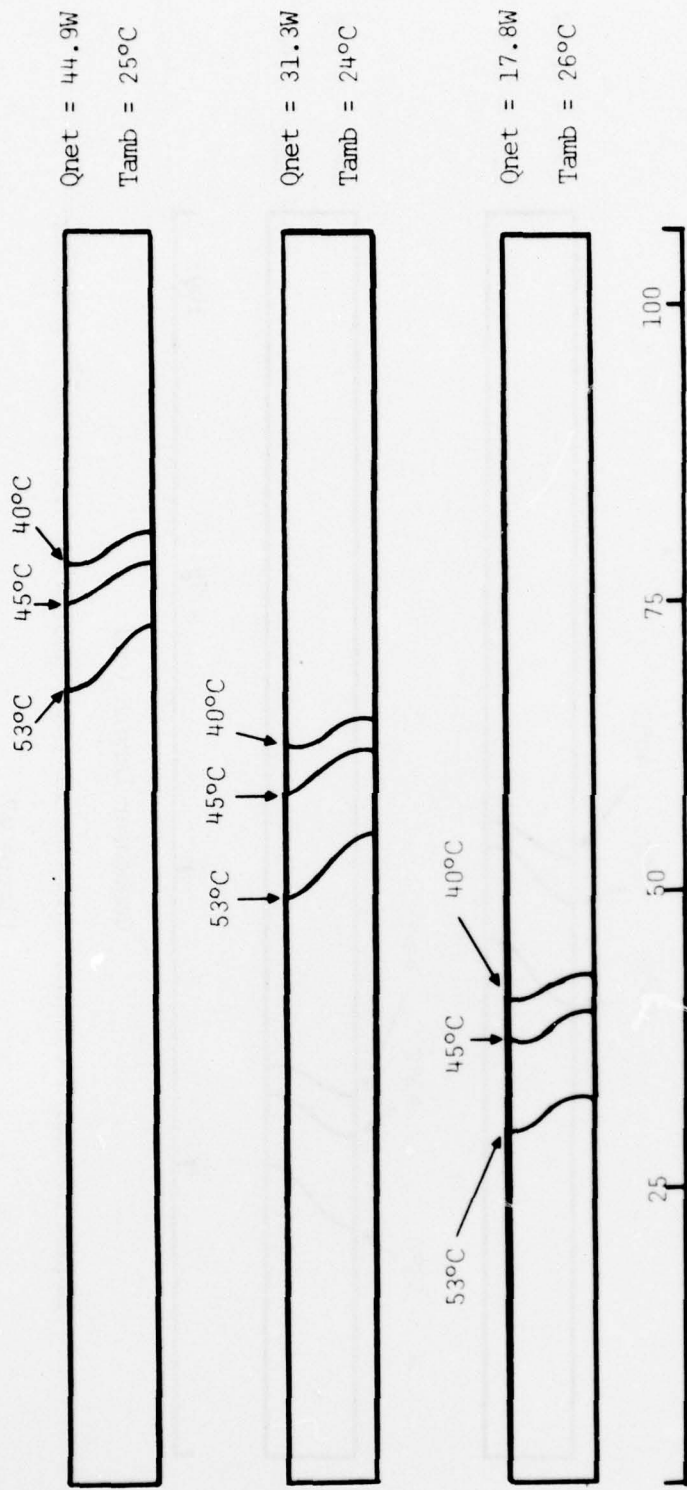
Figure 24

Qnet =	17.5W	31.7W	46.5W
Tamb =	27°C	25°C	25°C



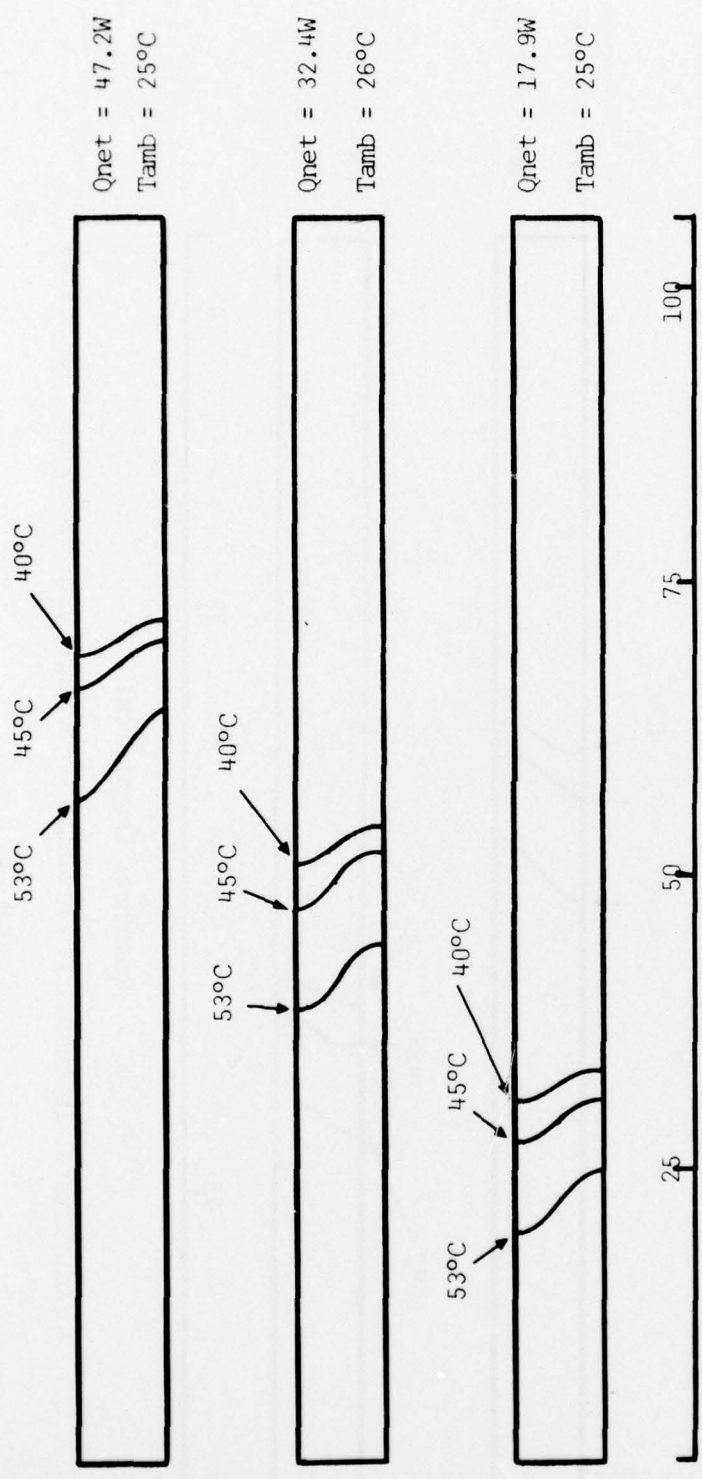
Liquid Crystal Isotherms; - Vertical Methanol with 1.59×10^{-3} kg Krypton

Figure 25



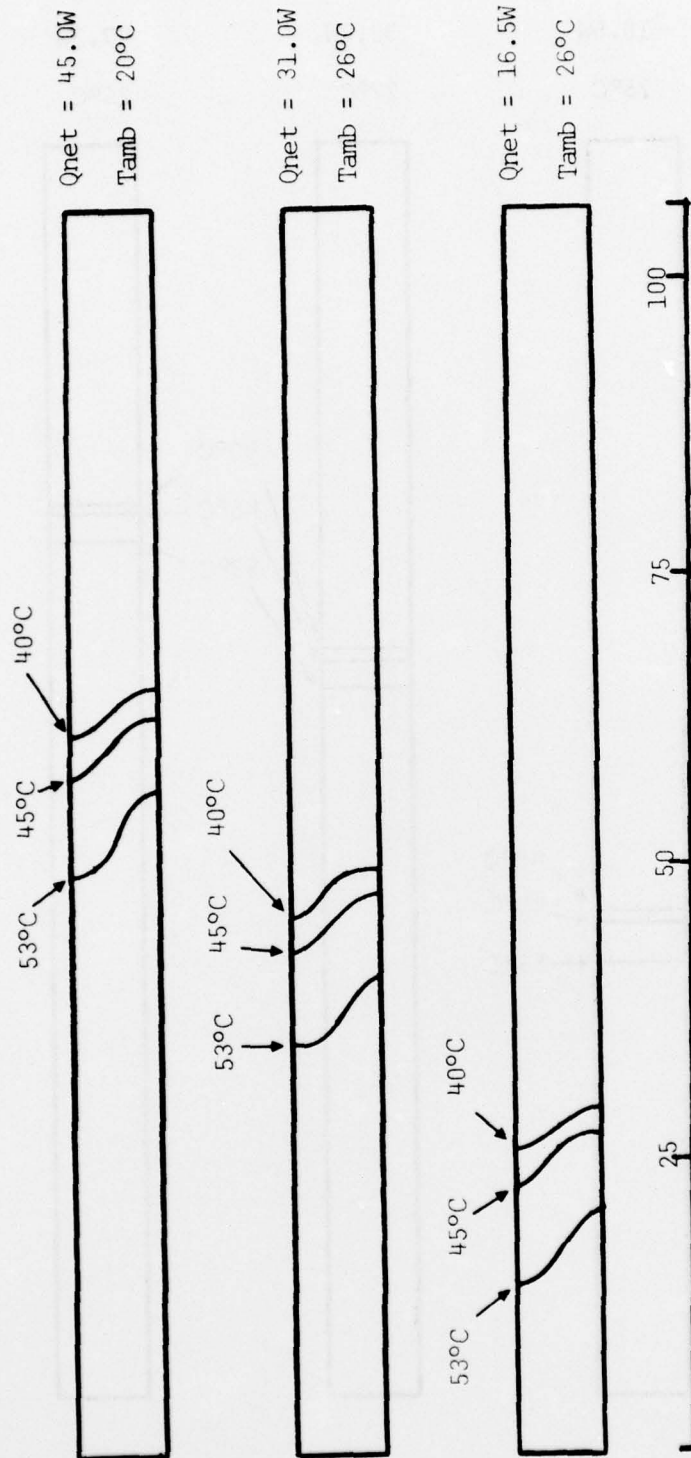
Liquid Crystal Isotherms - Horizontal - Methanol with 3.05×10^{-5} kg Helium

Figure 26



Liquid Crystal Isotherms - Horizontal - Methanol with 6.17×10^{-5} kg Helium

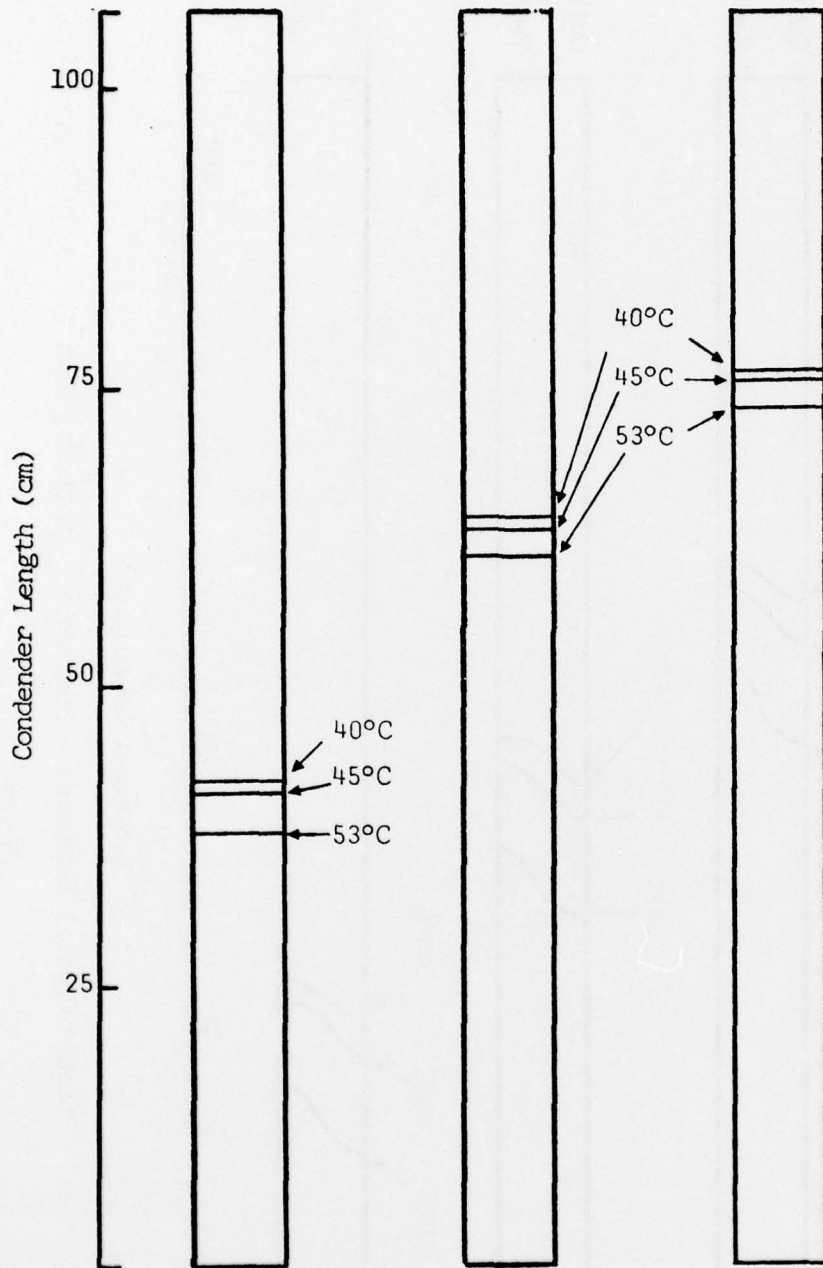
Figure 27



Liquid Crystal Isotherms - Horizontal - Methanol with 1.24×10^{-4} kg Helium

Figure 28

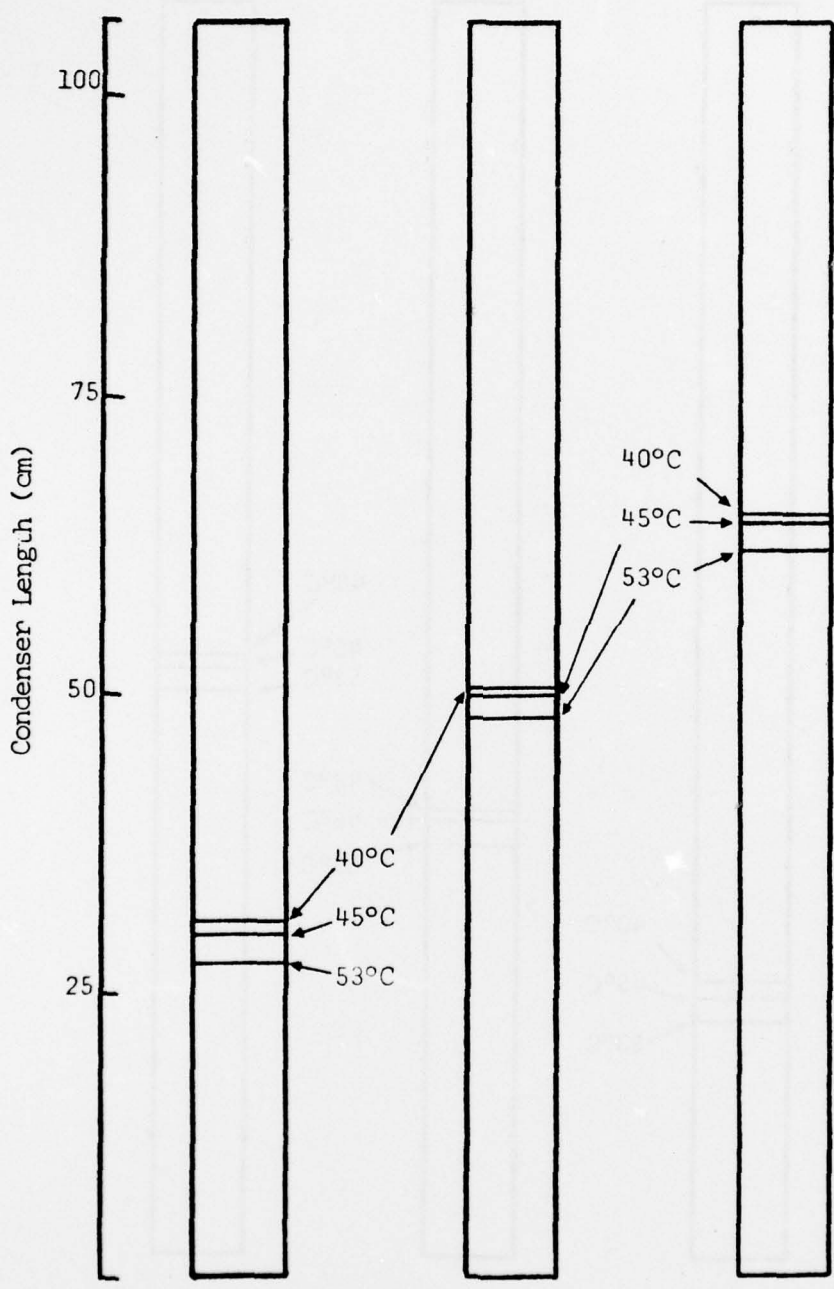
Qnet =	18.5W	32.2W	47.3W
Tamb =	25°C	27°C	25°C



Liquid Crystal Isotherms₅ - Vertical Methanol with 3.05×10^{-5} kg Helium

Figure 29

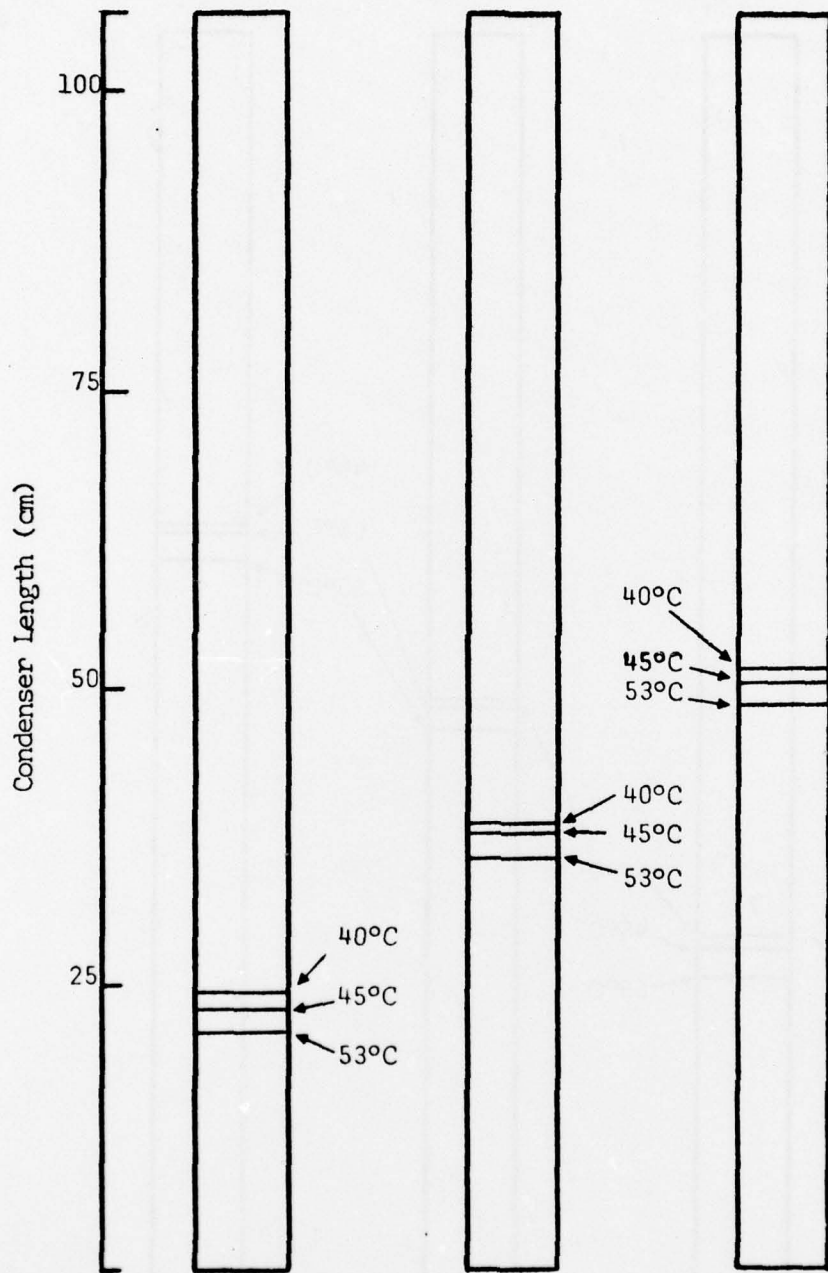
Qnet =	18.2W	32.2W	47.0W
Tamb =	23°C	25°C	24°C



Liquid Crystal Isotherms₅ - Vertical
Methanol with 6.17×10^{-5} kg Helium

Figure 30

Q _{net} =	16.9W	31.4W	45.9W
T _{amb} =	26°C	26°C	26°C



Liquid Crystal Isotherms_s - Vertical
Methanol with 1.24×10^{-4} kg Helium

Figure 31

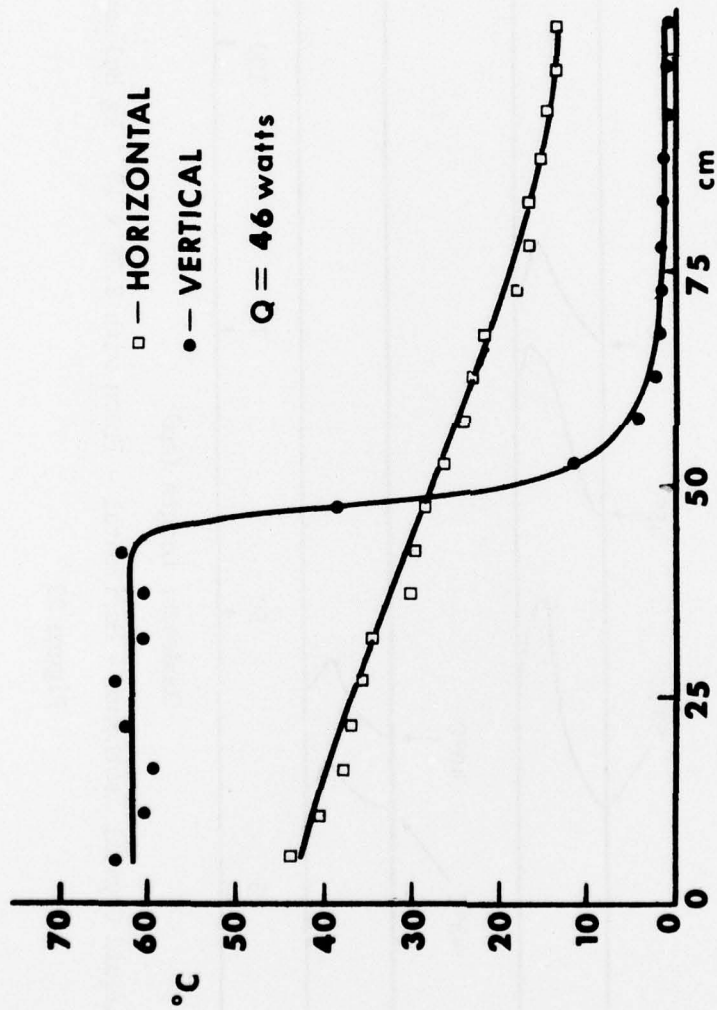
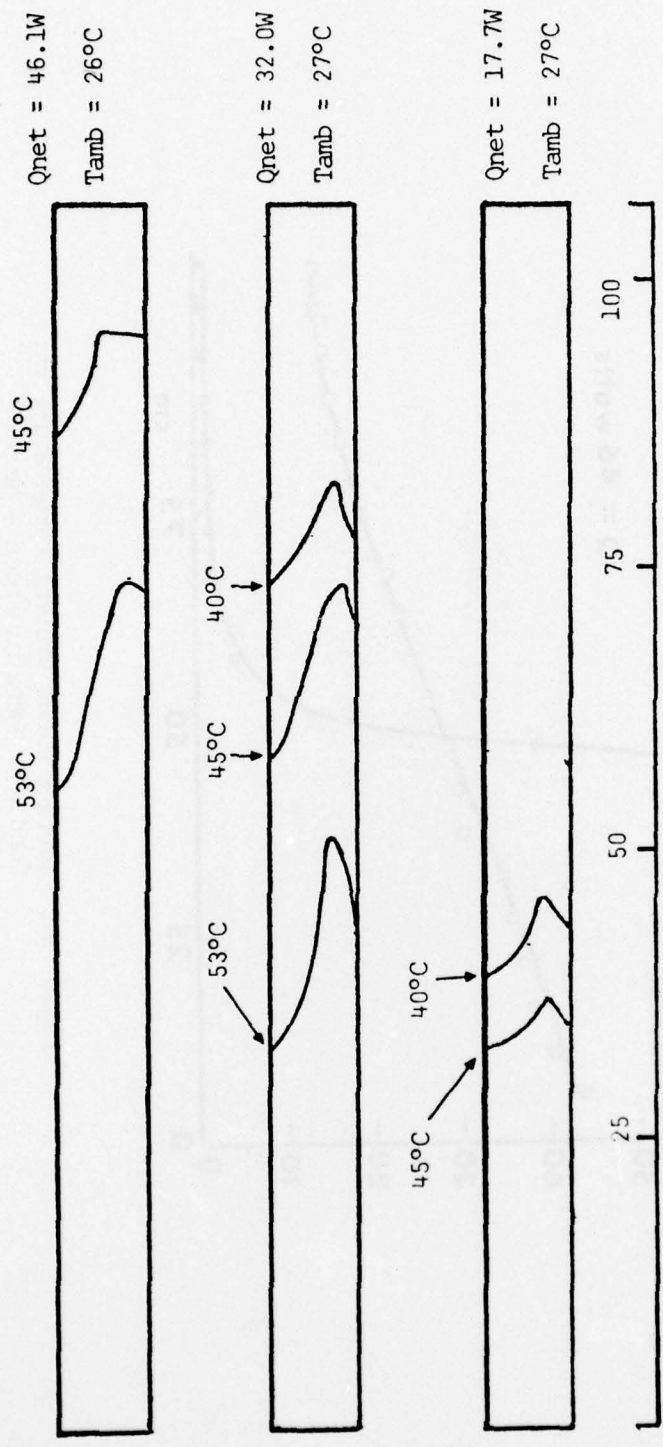
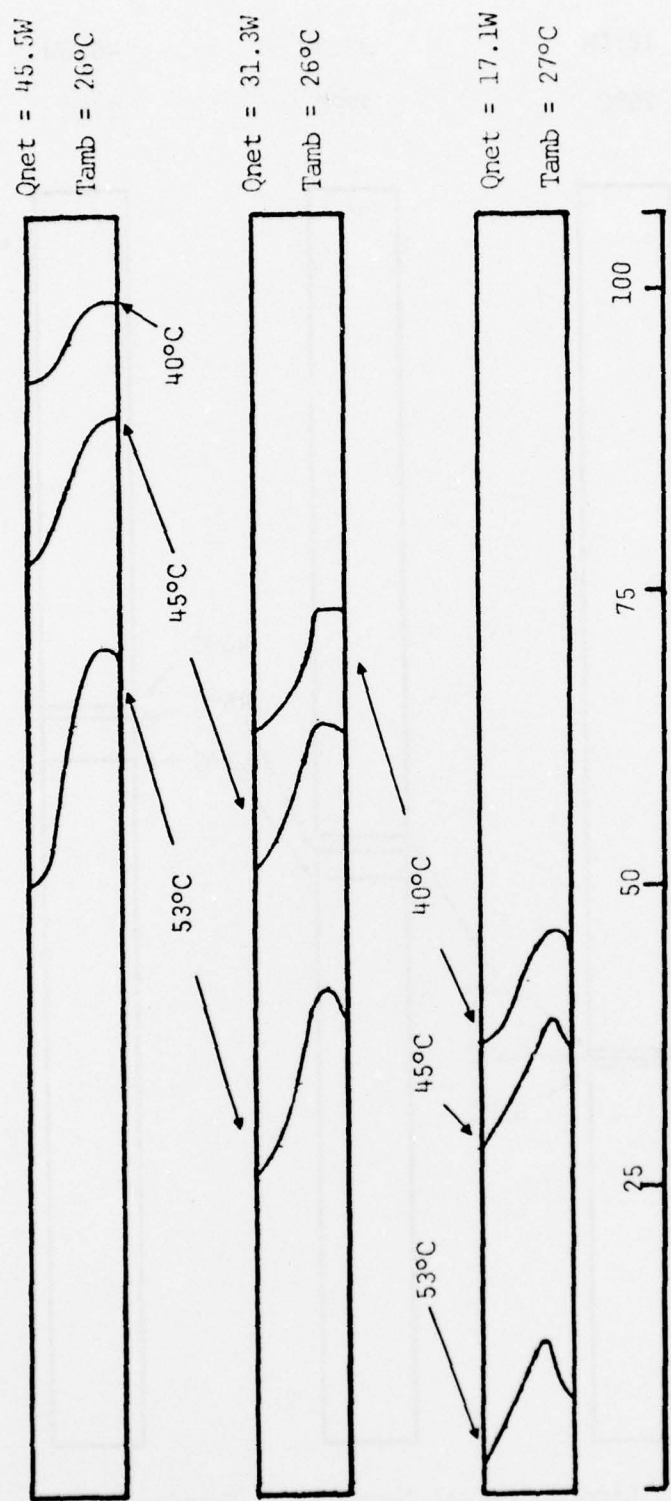


Figure 32. Surface minus ambient temperature vs.
 Condenser Length; Freon - Helium
 (Heat Pipe No. 2)



Liquid Crystal Isotherms - Horizontal - Freon with 8.26×10^{-5} kg Helium

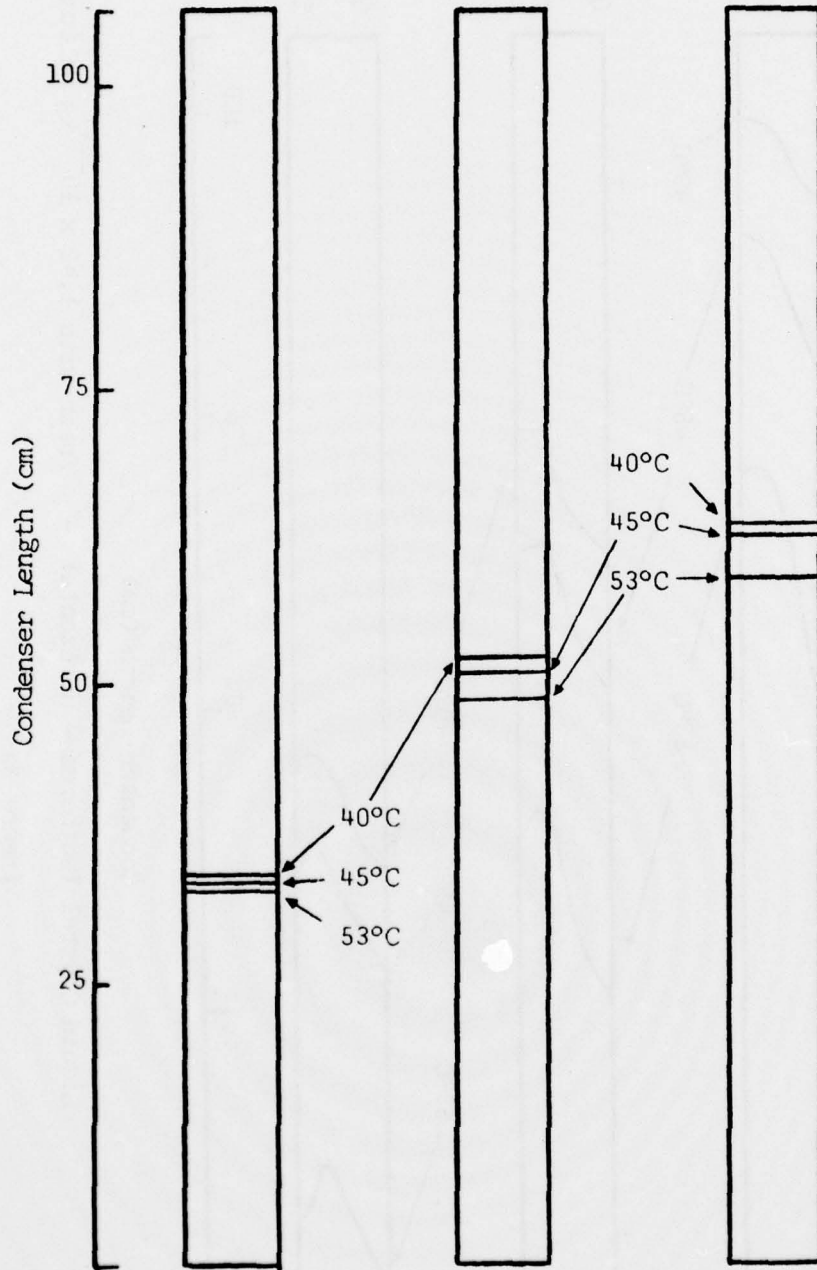
Figure 33



Liquid Crystal Isotherms - Horizontal - Freon with 1.42×10^{-4} kg Helium

Figure 3/4

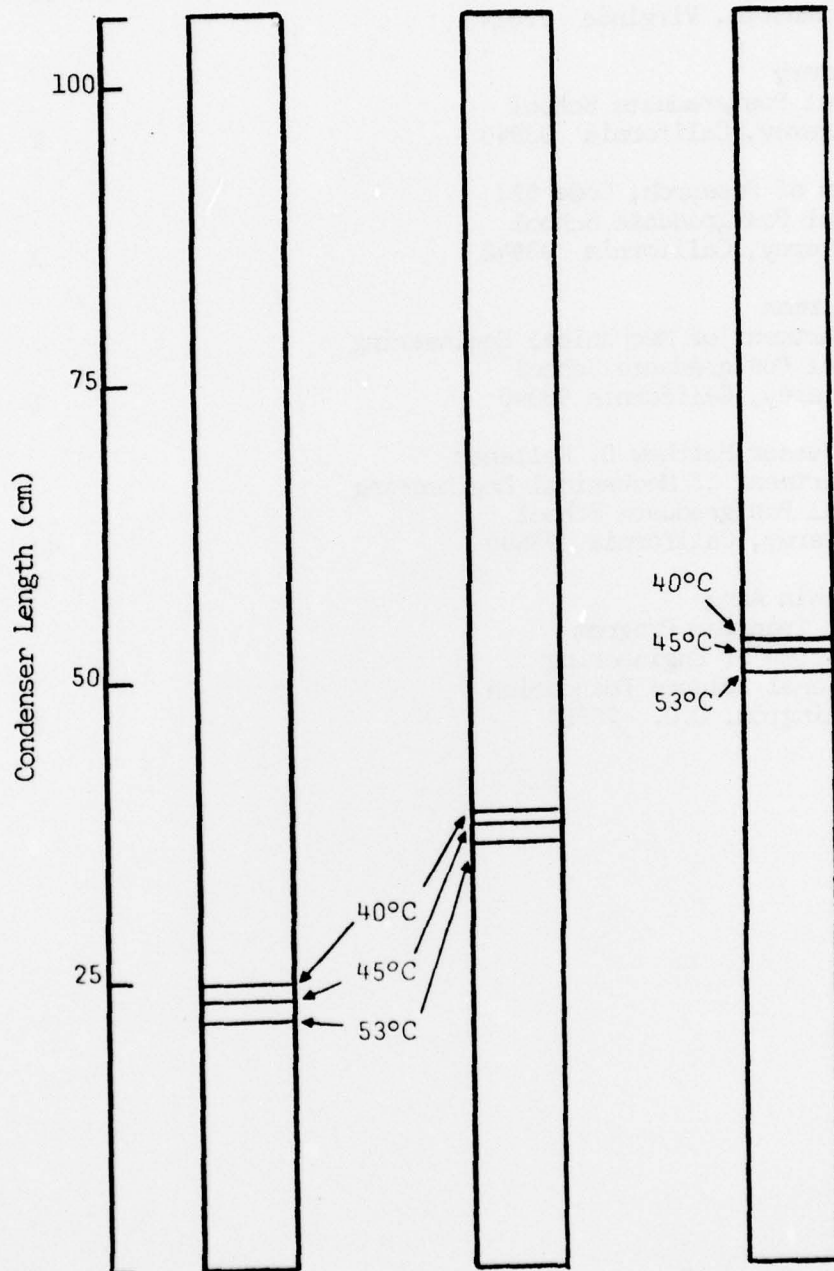
Qnet =	18.0W	32.3W	46.8W
Tamb =	26°C	27°C	27°C



Liquid Crystal Isotherms - Vertical
 Freon With 8.26×10^{-5} kg Helium

Figure 35

Qnet =	17.4W	31.7W	46.4W
Tamb =	27°C	27°C	27°C



Liquid Crystal Isotherms - Vertical
 Freon With 1.42×10^{-4} kg Helium

Figure 36

INITIAL DISTRIBUTION LIST

	<u>No. Copies</u>
1. Defense Documentation Center Cameron Station Alexandria, Virginia 22314	12
2. Library Naval Postgraduate School Monterey, California 93940	2
3. Dean of Research, Code 023 Naval Postgraduate School Monterey, California 93940	1
4. Chairman Department of Mechanical Engineering Naval Postgraduate School Monterey, California 93940	1
5. Professor Matthew D. Kelleher Department of Mechanical Engineering Naval Postgraduate School Monterey, California 93940	40
6. Dr. Win Aung Heat Transfer Program Division of Engineering National Science Foundation Washington, D.C. 20550	2